JOC The Journal of Organic Chemistry

Featured Article

Synthesis of Benzoxazoles Using Electrochemically Generated Hypervalent Iodine

Olesja Koleda, Timo Broese, Jan Noetzel, Michael Roemelt, Edgars Suna, and Robert Francke

J. Org. Chem., **Just Accepted Manuscript** • DOI: 10.1021/acs.joc.7b01686 • Publication Date (Web): 11 Aug 2017

Just Accepted

ACS Publications

The Journal of Organic Chemistry is published by the American Chemical Society.
1155 Sixteenth Street N.W., Washington, DC 20036

Synthesis of Benzoxazoles Using Electrochemically Generated Hypervalent Iodine

Olesja Koleda,[†] Timo Broese,[‡] Jan Noetzel,[§] Michael Roemelt,*[§∥] Edgars Suna*[†] and Robert Francke*[‡]

[†] Latvian Institute of Organic Synthesis, Aizkraukles 21, LV-1006, Riga, Latvia

[‡] Institute of Chemistry, Rostock University, Albert-Einstein-Str. 3a, 18059 Rostock, Germany

[§] Lehrstuhl für Theoretische Chemie, Ruhr-University Bochum, 44780 Bochum, Germany

[∥] Max-Planck Institut für Kohlenforschung, Kaiser-Wilhelm Platz 1, 45470, Mülheim an der Ruhr, Germany

michael.roemelt@theochem.ruhr-uni-bochum.de, edgars@osi.lv, robert.francke@uni-rostock.de

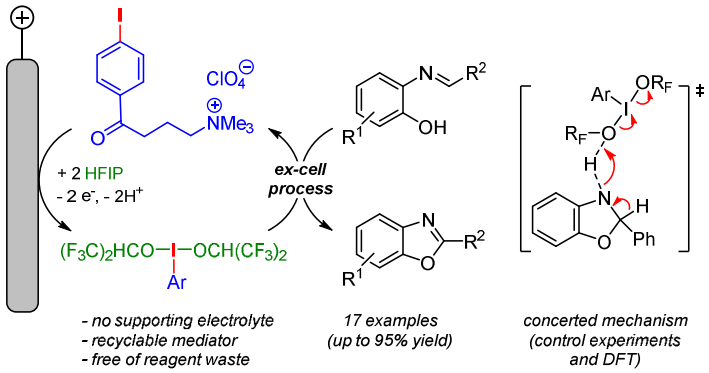

Abstract. The indirect ("*ex-cell*") electrochemical synthesis of benzoxazoles from imines using a redox mediator based on the iodine(I)/iodine(III) redox couple is reported. Tethering the redox active iodophenyl subunit to a tetra alkylammonium moiety allowed for anodic oxidation to be performed without supporting electrolyte. The mediator salt can be easily recovered and reused. Our "*ex-cell*" approach toward the electrosynthesis of benzoxazoles is compatible with a range of redox sensitive functional groups. An unprecedented concerted reductive elimination mechanism for benzoxazole formation is proposed on the basis of control experiments and DFT calculations.

Keywords: electrochemistry, hypervalent iodine, benzoxazole, reaction mechanism, density functional theory (DFT).

INTRODUCTION

Aryliodonium species constitute a versatile and efficient class of reagents with numerous applications in carbon-carbon and carbon-heteroatom cross-coupling reactions,[1] in oxidative rearrangements[2] and as terminal oxidants in metal-catalyzed syntheses.[3] Stoichiometric amounts of pre-formed aryliodonium reagents are routinely employed in these oxidative transformations, resulting in co-production of aryl iodide by-product together with the target molecule. Synthetic approaches relying on the *in situ* generation of aryliodonium catalysts from sub-stoichiometric amounts of iodoarenes and terminal oxidants such as *m*-CPBA and Oxone have been recently developed to minimize the aryl iodide by-product and to reduce loadings of relatively expensive iodine(III) reagents.[4,5] Although the overall cost may be reduced by the catalytic process, terminal oxidants still remain the source of stoichiometric waste. Electrochemical synthesis provides an attractive solution to the waste reduction, the increase of atom economy and cost-efficiency, because inexpensive electric current is employed as the terminal oxidant for the generation of I(III) reagents from iodoarenes.[6,7] Further improvement of atom economy can be accomplished by recovery and electrochemical reoxidation of the iodoarene species. Surprisingly, there are only few examples of separation and multiple reuse of the redox-active iodoarene reagents. This has been achieved by covalent attachment of iodoarene subunits to task specific ionic liquids[8] or to a polymer support.[9] In addition, Francke and Broese have recently demonstrated that merging of the redox-active iodoarene subunit with a tetraalkyl ammonium moiety not only facilitated efficient separation and reuse of the iodoarene reagent, but also allowed for efficient electrochemical generation of I(III) reagent without added external supporting electrolyte.[10] Hence, the ionically tagged phenyl iodide served both as redox mediator and supporting electrolyte in direct oxidative C–N and C–C bond forming reactions.[10] As a part of our ongoing research on electrochemical synthesis of heterocycles,[11] we report herein an application of the recyclable I(III) mediator-electrolyte system for electrosynthesis of 2-substituted benzoxazoles.

Benzoxazole is frequently encountered in biologically active natural products[12] and pharmaceuticals.[13] Several marketed drugs such as benoxaprofen, caboxamycin, flunoxaprofen, tafamidis and pseudopteroxazole possess the benzoxazole subunit. Among a plethora of methods for synthesis of benzoxazoles,[14] electrochemical synthesis is one of the most appealing as it provides excellent atom economy and sustainability. For instance, benzoxazoles have been recently prepared by direct electrosynthesis of anilides under galvanostatic mode (eq 1).[15] The developed approach is operationally simple, however the method has been only demonstrated for substrates possessing specific substituents (F, Cl or MeO) *para* to aniline nitrogen. Anodic oxidation of 2-phenoxypirimidines followed by chemical reaction of cyclized cationic intermediate with piperidine provided an access to 2-aminobenzoxazoles (eq 2).[16] Unfortunately, this approach features decreased atom economy due to the need of post-electrochemical functionalization step. Direct electrochemical oxidation of imines is also possible (eq 3), however, it required addition of LiOMe to facilitate the formation of benzoxazoles.[17] The presence of the strongly basic methoxide decreases the functional group compatibility. Indirect electrosynthesis using redox mediators such as DDQ[18] or sodium iodide[19] allows for electrochemical generation of benzoxazole under considerably milder conditions (eq 3). However, stoichiometric additives such as carbonate buffer (in NaI mediated reaction) or 2,6-lutidine and supporting electrolyte (in DDQ mediated process) were necessary to accomplish the indirect electrosynthesis. Furthermore, relatively electron rich imines were only used in the oxidative cyclization (R=Me, Cl, see eq 3), and nitro-substituted imines were unreactive. Herein we report an alternative approach which is based on the electrochemical generation of I(III) mediator prior to the addition of imine ("*ex-cell*" process). Furthermore, the redox active I(III) mediator possesses a quaternary ammonium moiety, which serves as supporting electrolyte and facilitates separation and reuse of the redox-active salt. The developed "*ex-cell*" approach does not require any additives, the oxidative formation of benzoxazoles proceeds under very mild conditions (room temperature) and the method is compatible with a broad range of functional groups as will be demonstrated below.[20]

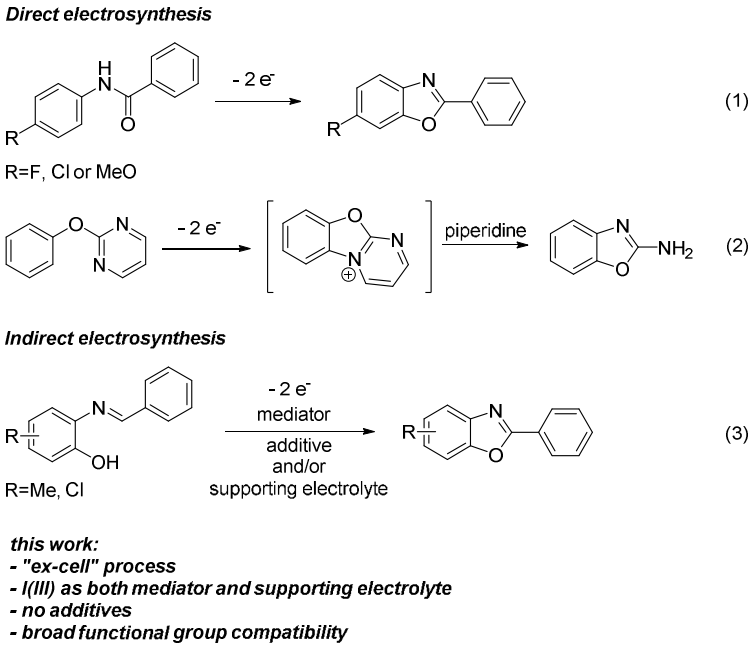

RESULTS AND DISCUSSION

Mediator properties. For the electrochemical generation of **2** from iodoarene **1**, previously reported optimized electrolysis parameters were applied (j = 15 mA cm^{-2}, Q = 1 F per mole **1**, [**1**] = 0.2 M, rt).[10] Due to its excellent anodic stability and its ability to stabilize iodine(III) species, the choice of 1,1,1,3,3,3-hexafluoroisopropanol (HFIP) as a solvent for electrolysis turned out to be the key to a successful oxidation of iodoarene **1** to **2** (Figure 1).[10] Unfortunately, the exact structure of the electrochemically prepared I(III) reagent **2** could not be determined because it undergoes decomposition as soon as HFIP is removed, and all attempts to isolate **2** in a pure form were not successful. The ^{1}H-NMR spectrum of HFIP solution of **2** (acquired immediately after electrolysis with added 50 vol % CH_2Cl_2–d_2) shows signals corresponding to parent aryl iodide **1** (δ 7.95 and 7.67 ppm) together with a downfield-shifted *para*-substituted aromatic spin system (δ 8.28 and 8.13 ppm; see Figure 1). The downfield signals were assigned to the aromatic subunit of I(III) reagent **2** based on similarity between ^{1}H and ^{13}C chemical shift values with those of hypervalent iodonium species **3** and **4**, prepared by chemical methods (Figure 1). Additional indirect support for the electrochemical formation of the I(III) reagent was

obtained in a control experiment where electrochemically prepared HFIP solution of I(III) reagent **2** effected clean oxidation of hydroquinone to 1,4-benzoquinone within 15 min at room temperature. Importantly, I(III) reagent **2** resulting from anodic oxidation of **1** is stable in HFIP *solution* at room temperature for several days (entry 1, Table 1). The observed stability of **2** is unusual because hypervalent I(III) species have been reported to oxidize secondary alcohols to the corresponding ketones.[21] In fact, relatively fast reduction of I(III) reagent **3** to aryl iodide **5** (ca. 40% after 15 min and ca. 65% after 20 h) with concomitant oxidation of HFIP to hexafluoroacetone (as evidenced by appearance of a signal at –82.9 ppm in ^{19}F spectrum) was observed at room temperature (eq 1, Figure 1.).

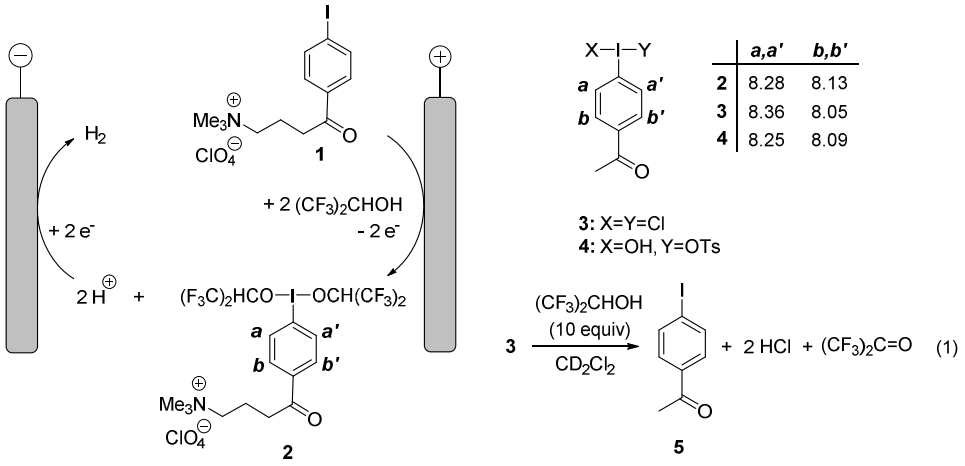

Figure 1. Indirect anodic oxidation of **1** to **2** in HFIP (15 mA cm^{-2}; WE – glassy carbon; CE – Pt sheet).

Several control experiments were performed to gain a better understanding of the unusual stability of the electrochemically generated I(III) species **2** and the observed facile decomposition of structurally related λ^3-iodane **3** in HFIP solution (eq 1, Figure 1). We reasoned that formation of HCl in the ligand exchange between **3** and HFIP could facilitate reductive elimination of **3** to iodoarene **5** and hexafluoroacetone (Figure 1, eq 1). Indeed, addition of anhydrous HCl to electrochemically generated **2** resulted in rapid formation of aryl iodide **1** (entry 2, Table 1). The nature of the anion in the acid is more important than the acidity of the proton, as evidenced by considerably slower conversion of **2** to **1** in the presence of sulfuric acid (entry 3). Furthermore, addition of excess Bu_4NCl (10 equiv) as a chloride

source triggered the reductive elimination of **2** to **1** under essentially neutral conditions (entry 4). Importantly, other halide anions were much more efficient (entries 5–7) with iodide effecting the most rapid decomposition of **2** (entry 7).[22] Addition of stoichiometric TEMPO did not affect the iodide-mediated conversion of **2** to **1** (entry 8), ruling out the reductive decomposition of **2** via a radical chain process. Finally, stability of the electrochemically generated **2** in the presence of added tertiary amine base (entry 10) as well as in the presence of a non-nucleophilic hydrogen sulfate additive (entry 9) led us to propose that nucleophilic reactivity of added halides is responsible for conversion of **2** to **1**. Hence, a plausible mechanism for halide anion-facilitated reductive decomposition of **2** is proposed involving addition of halide anion X to **2** to form equilibrating isomers of tetra coordinated [12-I-4] iodate **6** (scheme in Table 1).[23] Subsequent *intramolecular* β-elimination results in the oxidation of HFIP and concomitant reduction of I(III) species to iodoarene **1**.[24] The stability of electrochemically generated iodonium (III) species **2** apparently is attributed to the lack of nucleophilic ligands in the electrolyte. Hence, electrosynthesis opens the door for preparation of new hypervalent I(III) species that are difficult to access using chemical methods such as oxidation or ligands exchange.[25]

Table 1. Stability of electrochemically generated I(III) species **2**.

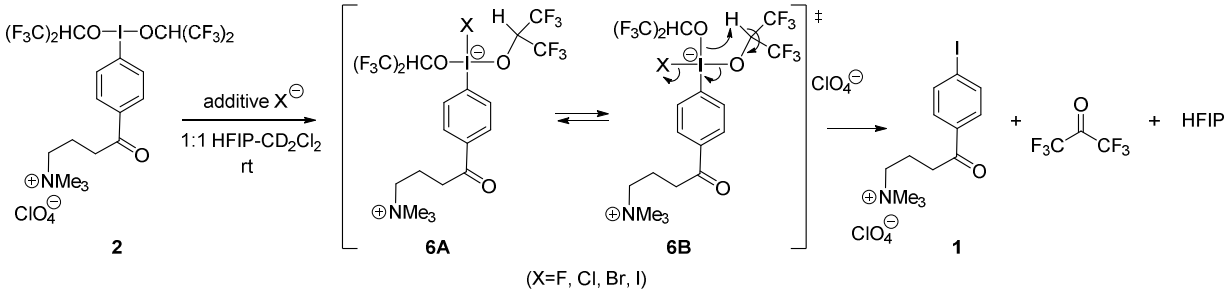

entry	additive (equiv.)	time	**1**, %[a]	conv. **2**, %[a]
1	none	10 days	12[b]	12
2	anhydrous HCl (1.4)	5 min	20[c]	76[c,d]
3	H_2SO_4 (1.4)	60 min	12[c]	12[c]

4	Bu_4NCl (10)	10 min	15	36[d]
5	Bu_4NF (10)	10 min	61	61
6	Bu_4NBr (10)	10 min	76	76
7	Bu_4NI (10)	10 min	86	86
8	1:1 Bu_4NI/TEMPO (1)	10 min	44	44
9	Bu_4NHSO_4 (10)	24 h	12	12
10	DIPEA (1)	24 h	6	6

[a] Determined by ^{1}H–NMR using 1-methyl-1*H*-pyrrole-2,5-dione as internal standard. [b] Electrochemically generated solution of **2** was stored at +4 °C. [c] CH_2Cl_2 was employed as the internal standard. [d]Inseparable mixture of unidentified side-products was also formed.

Benzoxazole synthesis. Next, the electrochemically generated I(III) reagent **2** was employed for oxidative cyclization of 2-(benzylideneamino)phenol **7** to benzoxazole **8**. The redox couple **1**/**2** has a higher oxidation potential (E_P(**1**) = 2.2 V vs. Ag/$AgNO_3$) as compared to that of imine **7** ((E_P(**7b**) = 0.8 V vs. Ag/$AgNO_3$).[26] Therefore, electrochemical generation of redox-mediator **2** in the presence of **7** (an "*in-cell*" process) is not possible, because in this scenario the phenolic substrate **7** would be oxidized before iodoarene **1**. Consequently, imine **7** has to be added to the electrolyte after completed anodic conversion of **1** to **2** (an "*ex-cell*" process). Indeed, addition of imine **7a** to electrochemically generated stoichiometric amounts of I(III) mediator **2** afforded 2-phenyl benzoxazole **8a** (Figure 2) in 87% yield (3.3 F/mole of passed charge with regard to the substrate **7a**). The I(III)-mediated „*ex-cell*" electrochemical cyclization is compatible with a broad range of functional groups in substrates such as alkene moiety (**7f,g,i**), bromine (**7b,o,q**), nitro group (**7c,m,o,p**),[27a] ether moiety (**7e,f,p**), ester (**7n**) and even carboxylic acid (**7q**). A variety of imines derived from non-enolizable aldehydes such as electron-rich (**7d**–**g**,**p**) and electron-deficient (**7c**) aromatic aldehydes, pyridyl-2-aldehyde (**7h**), cinnamaldehyde (**7i**) and pivalic aldehyde (**7j**) are suitable for the I(III)-mediated cyclization (Figure 2). The formation of benzoxazoles is not sensitive to steric hindrance in the imine moiety because *ortho*-substituted imines

(**7c**,**d**,**f,g**) undergo facile oxidative cyclization (Figure 2).[27b] It should be noted that simple ester hydrolysis in benzoxazole **8n** leads to the formation of the FDA-approved drug Tafamidis.[28] Benzoxazoles **8** can be also synthesized in a one-pot sequential two-step process from *ortho*-aminophenol and non-enolizable aldehyde without isolation of intermediate imine **7**. Accordingly, addition of I(III) mediator **2** to the *in situ* formed imine **7b**,**j** furnished the corresponding benzoxazoles in high yields (Figure 2). Finally, both HFIP and **1** can be recovered after completion of the cyclization. After HFIP removal by distillation, the redox-active iodoarene **1** possessing the tetraalkyl ammonium moiety can be recovered and purified by dissolving the solid residue in acetone followed by precipitation upon addition of diethyl ether (typical recovery yield is 90–95%).

Figure 2. Scope of substrates.

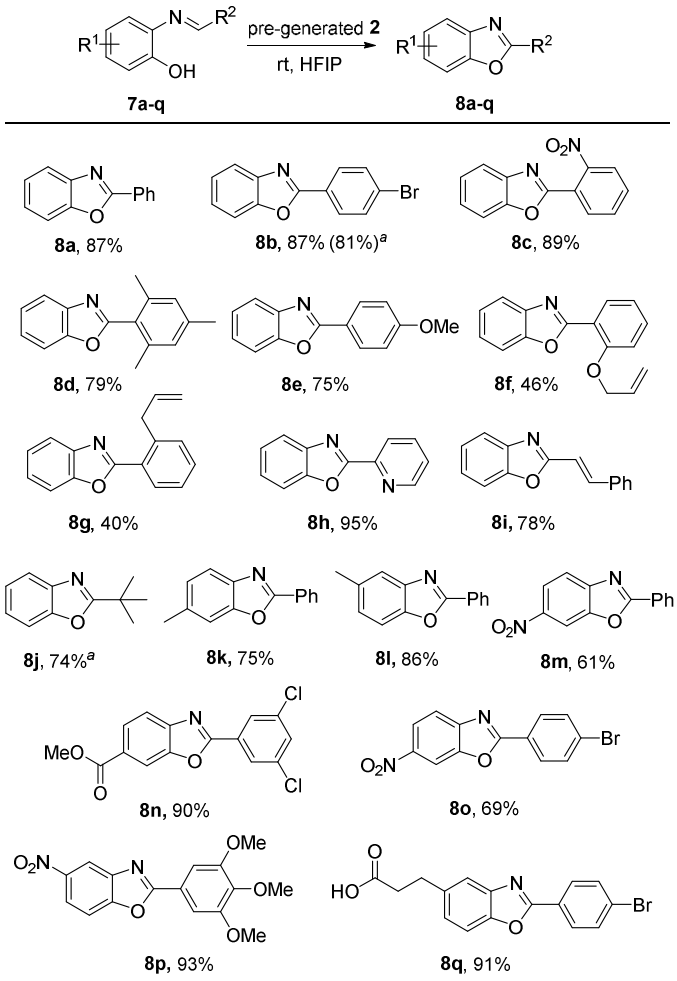

[a] Yield of sequential one-pot two-step synthesis.

Mechanistic studies. A series of control experiments have been carried out to elucidate the mechanism of benzoxazole formation. First, a single-electron transfer (SET) from relatively electron-rich arene **7a–A** to λ^3-iodane **2** was considered as a possible mechanistic scenario (pathway A, Figure 3).[29] The formed radical cation intermediate **IIa,b** would undergo another SET to form nitrenium-type species **IVb** affording benzoxazole **8a** upon loss of a proton (Figure 3). A radical inhibition test was performed to examine the possibility of benzoxazole formation via the SET pathway. Accordingly, the reaction of **7a–A** with **2** was performed in the presence of added radical scavengers such as TEMPO[30] (1 equiv) or *N*-*tert*-butyl-α-phenyl nitrone[5b] (1 equiv). However, neither of the additives influenced the yield of benzoxazole **8a** (87% yield in both cases; see Figure 2).

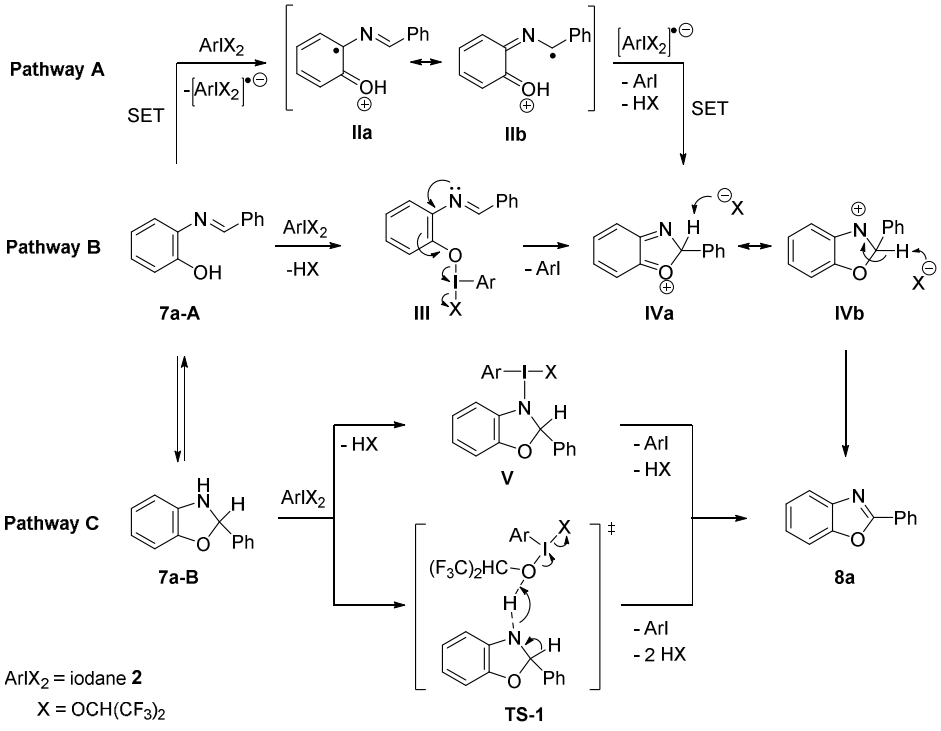

Figure 3. Plausible pathways for benzoxazole formation.

Next, imine **7g** containing an *ortho*-allyl moiety as a radical clock probe was employed to test for the intermediacy of radical cation species such as **II** in the synthesis of benzoxazoles (Figure 4). Based on

the analogy with a previous study on the cyclization of 2-allylbenzyl radicals where a rapid 5-*exo*-*trig* cyclization was reported (rate constant $k = 3 \times 10^2$ s^{-1}),[31] one would expect the formation of 2-methyl-2,3-dihydro-1*H*-indene **VI** after abstraction of a hydrogen atom from the medium (eq 1, Figure 4). However, in our hands, benzoxazole **8g** was obtained as the major product, and no detectable amounts of the cyclization product **VI** were observed (eq 2, Figure 4). These data provide an evidence that the I(III)-mediated benzoxazole formation occurs without involvement of benzyl radicals such as **IIb** (pathway A, Figure 3).

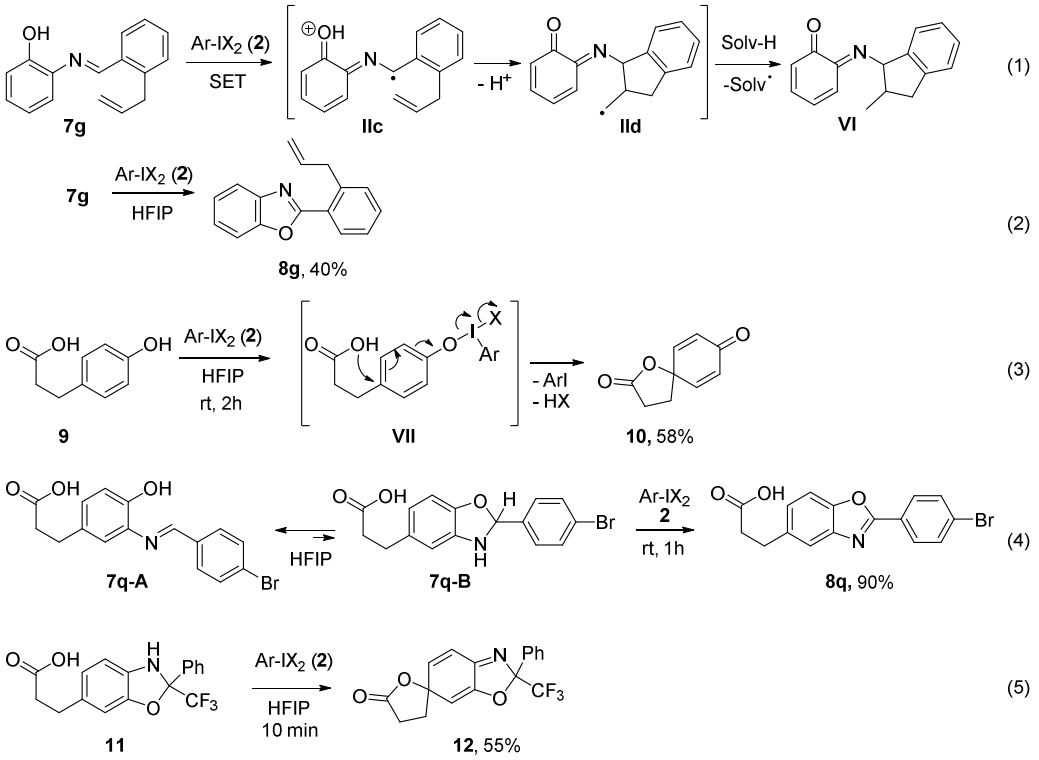

Figure 4. Control experiments.

In an alternative possibility, pathway B involves reaction of nucleophilic phenolic oxygen with **2** in a ligand-exchange process to form aryloxy-λ^3-iodane **III**. Decomposition of **III** via oxidation of the phenol followed by cyclization would afford intermediate **IV**, which is transformed into benzoxazole **8a** upon loss of a proton (Figure 3). To verify the intermediacy of aryloxy-λ^3-iodane **III** in the benzoxazole formation, substrates **7q** and **9** that contain a propionic acid moiety *para* to the phenolic oxygen were synthesized (eq 3 and 4, Figure 4). It is well-known that the tethered carboxylic acid is suitable as a

nucleophile for intramolecular trapping of phenol oxidation products, derived from fragmentation of transient aryloxy-λ^3-iodanes.[32] Indeed, electrochemically generated I(III) reagent **2** reacted with phenol **9** to form spirocycle **10** within 3h at rt (eq 3, Figure 4). In sharp contrast, structurally related **7q** was converted to benzoxazole **8q** under similar conditions (2 h, rt, 90% yield) and none of the spirocyclization products could be observed in the reaction mixture (eq 4, Figure 4). Hence, the involvement of aryloxy-λ^3-iodane **III** in the formation of benzoxazoles can be questioned.

As a third option, pathway C involves equilibrium formation of cyclic hemiaminal **7a**–**B** from imine **7a**–**A**. Cyclic tautomer **7a**–**B** reacts with I(III) species **2** to form a new hypervalent iodine (III) intermediate **V**,[33] which undergoes reductive elimination of Ar-I to form **8a**. Alternatively, benzoxazole **8a** can be formed directly from cyclic hemiaminal **7a**–**B** by a concerted reductive elimination via transition state **TS-1** (Figure 3). Although cyclic hemiaminal **7a**–**B** has not been observed by NMR methods in a 1:1 HFIP-CD_2Cl_2 solution of imine **7a**–**B** (only signals at δ=8.67 (^{1}H–C=N) and δ=159.1 (^{13}C=N) could be seen), its equilibrium formation cannot be excluded. Furthermore, the cyclic tautomer **7a**–**B** may react with I(III) reagent **2** considerably faster than does imine **7a**–**A** (Curtin-Hammett conditions). In fact, such a scenario is in agreement with the observed distinct reactivity of phenols **7q**–**A** and **9** with I(III) reagent **2** (eq 3 and 4, Figure 4). To verify the involvement of the cyclic tautomer **7a**–**B** in the benzoxazole formation, structurally related ketimine **11** with tethered carboxylic acid was synthesized. As anticipated, NMR spectra of ketimine **11** in 1:1 HFIP-CD_2Cl_2 solution only showed the presence of the cyclic hemiaminal tautomer (evidenced by ^{13}C signal at δ = 98.7, J = 32.2 Hz). Notably, clean transformation of ketimine **11** to spirocycle **12** (as a 1:1 mixture of diastereomers) was observed upon addition of I(III) reagent **2** under standard conditions (HFIP, rt, 10 min, 55% yield; see eq 5, Figure 4). Facile formation of spirocycle **12** from the cyclic ketimine **11** and the absence of spirocyclization products for the non-cyclic aldimine **7q**–**A** renders the pathway C (Figure 3) as the most plausible mechanism of benzoxazole formation. Further support for pathway C as the most viable mechanistic

scenario as well as evidence in favor of the concerted reductive elimination (*via* transition state **TS-1**) as opposed to intermediate **V** in the pathway C were obtained by theoretical investigations as shown below.

Computational studies. The proposed reaction pathways B and C (Figure 3) have been probed by quantum chemical calculations on a model comprising substrate **7a**, iodine reagent **13**[34] and an additional solvent molecule (Figure 5). Technical details together with a description of the chosen theoretical approach are provided in the Experimental Section and the SI. Computed reaction pathway B involved transfer of a phenolic proton of **7a–A** to the HFIP ligand of mediator **13** to induce a ligand substitution at the I(III) center and formation of intermediate **III** (Figure 6). The substitution is computed to be exothermic by 5.6 kcal mol^{-1}. Furthermore, the corresponding transition state **TS-2** could be identified. It is associated with a reaction barrier of 7.2 kcal mol^{-1} and its reaction coordinate is dominated by the proton transfer from the substrate to the HFIP ligand. After the substrate is bound to the I(III) center, a reductive elimination from the iodine center triggers the ring closure to give intermediate **IVa,b**. The total reaction enthalpy for this step accounts to ΔG = -7.4 kcal mol^{-1} and is thus thermodynamically feasible. Unfortunately, despite intense efforts, the optimization of the corresponding transition state did not meet the convergence criteria. Nevertheless, our thorough search of the potential energy surface yielded a configuration with a single imaginary harmonic frequency that is associated with a symmetric mode of the iodine-oxygen bonds. Since such a motion eventually leads to the desired minima (as we have verified by separate relaxed surface scans), we strongly believe that the obtained structure resembles the true transition state. Thus, the obtained value of $\Delta G^{\ddagger}$ = 18.0 kcal mol^{-1} corresponding to **TS-3** is a reasonable approximation for the reaction barrier.

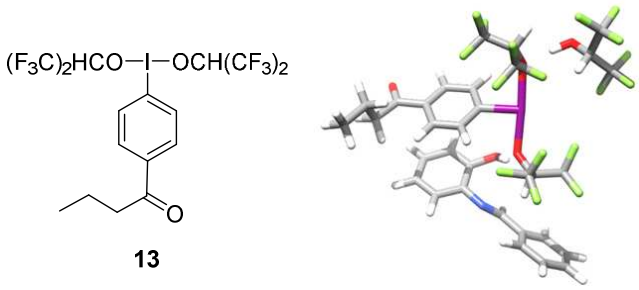

13

Figure 5. The model system containing iodine(III) species **13**, imine **7a** and an additional HFIP molecule.

At this point it should be noted that in order to obtain realistic reaction enthalpies for the reductive elimination, it is of great importance to explicitly include an additional solvent molecule (see Figure 5) that acts to stabilize the generated HFIP anion through formation of a strong hydrogen bond. Another important aspect of the explicit inclusion of a HFIP molecule is that it is required as structural aid during the ring closure. Without any solvent molecule in the vicinity of the imine group no ring closure is observed. After the solvent–induced ring annulation, the formed nitrenium cation **IV** is stabilized by the adjacent alkoxide ion (X^-). However, this ion pair **IVa,b** is metastable. When the HFIP anion is manually placed in the vicinity of the proton in α-position to the nitrenium ion, the proton is abstracted without a barrier resulting in the final product and a gain of ΔG = -41.1 kcal mol^{-1}. This manual procedure simulates a solvent mediated motion of the HFIP anion which we anticipate to readily occur at room temperature.[35] Alternatively, provided the concentration of mediator and substrate is sufficiently high, a HFIP anion from a neighboring reaction center could act as the required base. In both cases the final product is formed under considerable heat production.

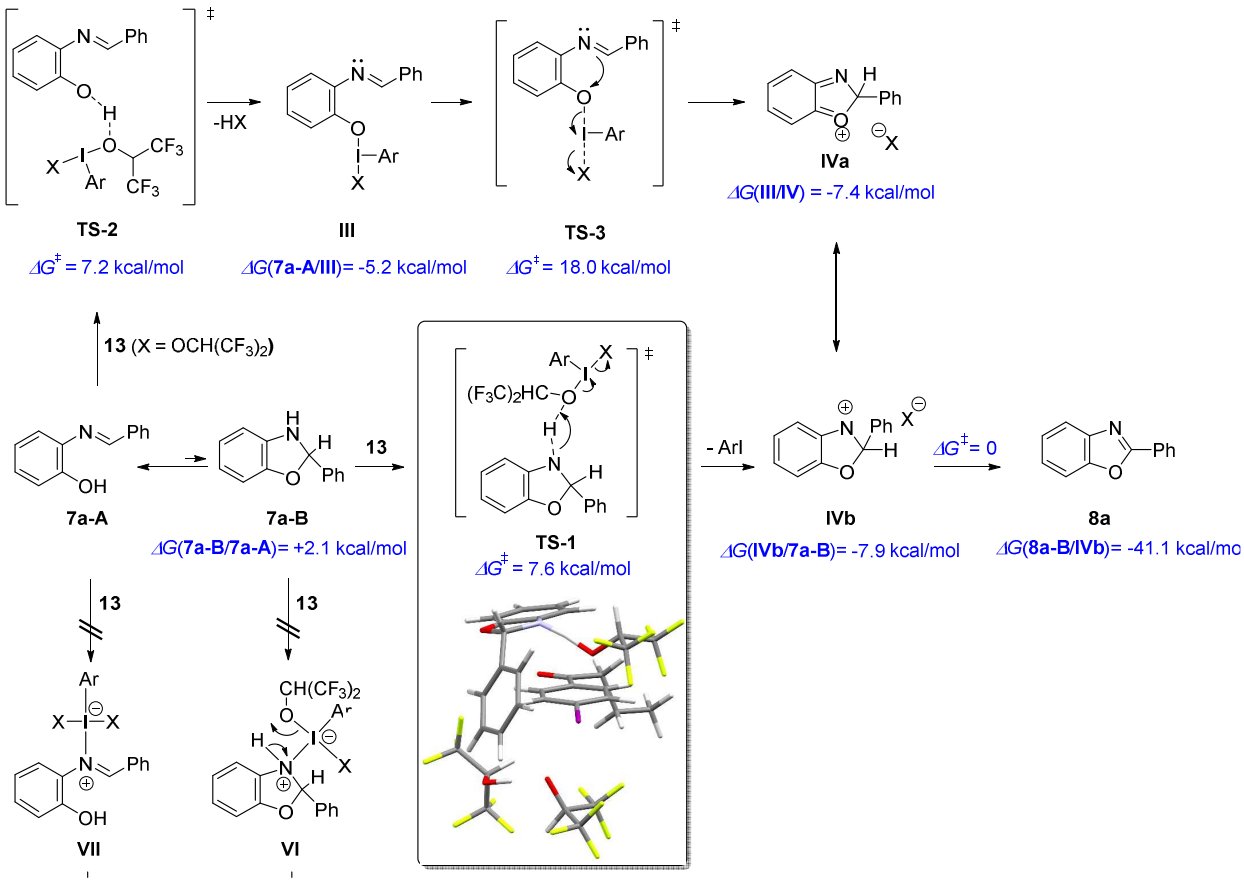

Figure 6. Summary of the computational results on the proposed pathways B and C (cf. Figure 3). The structure of transition state **TS-1** is inserted as sticks model (with iodine displayed violet, hydrogen white, carbon grey, oxygen red, nitrogen blue and fluorine green). The black arrows indicate the corresponding reaction coordinate which is dominated by the proton transfer from the substrate to its adjacent HFIP anion.

Next, theoretical investigations of the two alternative reaction coordinates (**TS-1** vs. intermediate **V**) in pathway C were performed (cf. Figure 3). Intermediate **V** can be formed from imine **7a**–**A** and **13** through tetracoordinated [12-I-4] iodate **VII**.[20a] However, stationary points on a potential energy surface corresponding to intermediate **VII** could not be found (Figure 6). Alternatively, I(III) reagent **13** may react with cyclic hemiaminal **7a**–**B** to form iodate **VI**, which loses a HFIP molecule to afford intermediate **V** (cf. Figure 3). The latter pathway involves cyclic hemiaminal **7a**–**B**, a species that could not be observed by ^{1}H-NMR methods (*vide supra*). Notably, our calculations indicate that the tautomerization of

imine **7a–A** to hemiaminal **7a–B** in the presence of I(III) species **13** is favored by 5.7 kcal mol^{-1} (see Figure 6). As the relative stability is reversed when the Gibbs free energies of **7a-A** and **7a-B** are calculated without **13** and an additional HFIP molecule (ΔG(**7a-A**/**7a-B**) = 2.1 kcal mol^{-1}) this suggests a possible stabilization of the cyclic hemiaminal tautomer by I(III) species **13**. In the meantime, calculations did not lead to stationary points on the potential energy surface corresponding to intermediate **VI**. Furthermore, intermediate **V** spontaneously undergoes reductive elimination when optimized with a solvent molecule in the vicinity of its hemiaminal part. Hence, lack of evidence for the formation of parent species **VI** and **VII** and its own instability puts in question the involvement of the key intermediate **V** in the pathway C for benzoxazole formation. Instead, we have found that pre-coordination through hydrogen bonding of N–H in **7a–B** with Lewis basic oxygen of the HFIP ligand in **13** triggers a concerted reductive elimination *via* **TS-1** to form iodoarene and ion pair comprising nitrenium cation **IVa**,**b** and a HFIP anion. The concerted reaction is exergonic with ΔG = –7.9 kcal mol^{-1} and it has a relatively low reaction barrier of $\Delta G^{\ddagger}$ = 7.6 kcal mol^{-1} (**TS-1**). Transition state **TS-1** exhibits elongated I–O bonds (2.69 Å and 2.72 Å), whereas the N–H and O–H bond lengths are 1.18 Å and 1.31 Å, respectively. Hence, it appears that at this point the reductive elimination is almost completed while the hydride transfer has yet to take place. Accordingly, the corresponding reaction coordinate is mainly composed of the hydride transfer movement accompanied by only a minor stretching of the I–O bonds (see stick model for transition state **TS-1** in Figure 6).

The computed reaction barrier corresponding to transition state **TS-1** ($\Delta G^{\ddagger}$ = 7.6 kcal mol^{-1}, pathway C) is considerably lower in energy as compared to that for **TS-3** ($\Delta G^{\ddagger}$ = 18.0 kcal mol^{-1}, pathway B). Hence, our computational results support the pathway C (Figure 3) as the most plausible mechanism for the observed oxidative cyclization as it involves only low kinetic barriers and each step is thermodynamically favorable. Among the two possible scenarios within the pathway C, our results strongly favor the concerted reductive elimination *via* transition state **TS-1** as the most likely mechanism for benzoxazole formation.

CONCLUSIONS

Anodic oxidation of iodoarenes in HFIP as a solvent allows for convenient preparation of I(III) species under essentially neutral conditions and at room temperature. The electrochemically generated dialkoxy-λ^3-iodane is stable as a solution in HFIP for more than a week at +4^o C (12% decomposition after 10 days). In the presence of nucleophilic anions such as halides, facile reductive elimination of I(III) species to the corresponding aryl iodide, hexafluoroacetone and HFIP takes place. Poor compatibility of dialkoxy-λ^3-iodanes with nucleophiles renders anodic oxidation a convenient alternative to the traditional approaches such as chemical oxidation or ligands exchange reaction for generation of HFIP-containing I(III) species. Addition of electrochemically generated I(III) species to *ortho*-imino phenols results in clean formation of benzoxazoles. The "*ex-cell*" electrochemical synthesis of benzoxazoles is compatible with a broad range of redox sensitive functional groups, including alkene, bromine and carboxylic acid. Benzoxazoles can be also synthesized in a one-pot sequential two-step process by addition of electrochemically generated I(III) oxidant to the *in situ* formed imines. Our combined experimental and theoretical approach suggests that oxidative cyclization of *ortho*-imino phenols to benzoxazoles proceeds through 2,3-dihydrobenzoxazole as the key intermediate. DFT studies of several conceivable pathways indicate that a sequence via a concerted reductive elimination represents the most plausible mechanistic scenario for the formation of benzoxazoles.

EXPERIMENTAL SECTION

General Information. Unless otherwise noted, all chemicals were used as received from commercial sources and all reactions were performed under nitrogen or argon atmosphere. Anhydrous CH_2Cl_2 was obtained by passing commercially available anhydrous solvents through activated alumina columns. Analytical thin-layer chromatography (TLC) was performed on pre-coated silica gel F-254 plates. Nuclear magnetic resonance spectra were recorded on NMR spectrometers at the following frequencies: ^{1}H, 400 or 300 MHz; ^{13}C{^{1}H}, 100.6, 75 or 63 MHz; ^{19}F, 376.3 MHz. Chemical shifts are reported in

parts per million (ppm) relative to TMS or with the residual solvent peak as an internal reference. High-resolution mass spectra (HRMS) were recorded on a mass spectrometer with a time-of-flight (TOF) mass analyzer using the ESI technique. Electrolysis was performed under galvanostatic control in an undivided cell. Glassy carbon (SIGRADUR G-plate, 10x50x5 mm) served as a working electrode; a Pt sheet (10x50x0.1 mm) served as a counter electrode.

Cyclic voltammetry. The experiments were carried out in a three-electrode cell using a glassy carbon disc (diameter: 3 mm) as a working electrode and a platinum wire as a counter electrode. The glassy carbon disc was polished using polishing alumina (0.05 μm) prior to each experiment. $Ag/AgNO_3$ electrode (silver wire in 0.1 M NBu_4ClO_4/CH_3CN solution; $c(AgNO_3)$ = 0.01 M) was used as a reference and this compartment was separated from the rest of the cell with a Vycor frit. 0.1 M solution of NBu_4ClO_4 (Electrochemical grade) in HFIP was used as electrolyte. The electrolyte was purged with argon for at least five minutes prior to recording the CVs.

***N*-[4-(4-Iodophenyl)-4-oxobutyl]-*N*,*N*,*N*-trimethylammonium perchlorate (1)** was synthesized in three steps from iodobenzene and 4-chlorobutanoyl chloride according to the procedure reported in the literature.[10] ^{1}H-NMR data are identical to those reported in the literature. ^{1}H NMR (400 MHz, DMSO, ppm) δ 7.96 – 7.94 (m, 2H), 7.75 – 7.72 (m, 2H), 3.33 – 3.29 (m, 2H), 3.12 (t, J = 6.8 Hz, 2H), 3.08 (s, 9H), 2.08 – 1.99 (m, 2H). $^{13}C\{^1H\}$ NMR (100.6 MHz, $CDCl_3$, ppm) δ 198.0, 137.7, 135.6, 129.6, 102.0, 64.7, 52.2, 34.4, 16.8. Anal. Calcd for $C_{13}H_{19}ClINO_5$: C, 36.17; H, 4.44; N, 3.24. Found: C, 36.25; H, 4.38; N, 3.21.

Procedure for the Electrochemical Generation of I(III) Reagent 2. The electrolysis in an undivided cell was performed following the procedure reported in literature.[10] A glassy carbon piece (immersed surface area: A = 1 cm^2) served as a working electrode, a platinum sheet – as a counter electrode. The experiment was carried out as follows: aryl iodide **1** (864 mg, 2 mmol) was dissolved in 1,1,1,3,3,3-hexafluoroisopropanol (HFIP, 10 mL) and molecular sieves (4Å, 2.0 g) were added. After purging the cell with argon, the clear solution was electrolyzed with a current density of 15 mA/cm^2 until charge 1 F per mol of **1** was passed. Upon completion of the electrolysis, an aliquot (0.3 mL) from the light-yellow

electrolysis solution was diluted with CD_2Cl_2 (0.3 mL). ^{1}H NMR analysis of the aliquot helped to determine the Faraday efficiency of 67% for the electrolysis. Accordingly, the concentration of the electrolysis solution was 0.67 M in **2**. ^{1}H NMR (400 MHz, CD_2Cl_2, ppm) δ 8.32 – 8.29 (m, 2H), 8.16 – 8.13 (m, 2H), 4.39 (septet, J = 5.9 Hz, 2H), 3.40 – 3.32 (m, 2H, the signal overlaps with those of **1**), 3.29 (t, J = 6.4 Hz, 2H), 3.17 (s, 9H), 2.31 – 2.19 (m, 2H, the signal overlaps with those of **1**). ^{13}C{^{1}H} NMR (100.6 MHz, CD_2Cl_2, ppm) δ 200.4, 140.0, 153.3, 132.0, 104.0 (the signal overlaps with those of **1**), 67.9, 54.7 (the signal overlaps with those of **1**), 35.5, 18.2. ^{19}F NMR (376.3 MHz, CD_2Cl_2) δ –75.07 (d, J = 5.8 Hz).

1-(4-(Dichloro-λ^3-iodanyl)phenyl)ethan-1-one (3) was synthesized according to the literature procedure.[36] Thus, 4'-iodoacetophenone (492 mg, 1 mmol) was dissolved in MeCN (4 mL) and aqueous 5.84% NaOCl solution (12 mL) was added, followed by the slow addition of aqueous concentrated HCl (4 mL). Light yellow precipitate was formed. After 20 min at room temperature the precipitate was filtered off and washed with H_2O and hexanes. Drying at room temperature overnight in the dark afforded the title compound **3** as a light yellow solid (620 mg, 98% yield). Pure material was obtained by recrystallization from hexanes/CH_2Cl_2, mp 76.5 – 75.5 ^{o}C (decomp.). ^{1}H NMR (400 MHz, CD_2Cl_2, ppm) δ 8.33 – 8.30 (m, 2H), 8.03 – 7.99 (m, 2H), 2.63 (s, 3H). ^{13}C{^{1}H} NMR (100.6 MHz, CD_2Cl_2, ppm) δ 196.7, 140.2, 134.6, 131.5. 129.5, 27.2. HRMS (ESI-TOF) *m/z*: $[M]^+$ Calcd for $C_8H_7ClIO^+$ 280.9230; Found 280.9234.

(4-Acetylphenyl)(hydroxy)-λ^3-iodanyl 4-methylbenzenesulfonate (4). To a stirred solution of 4'-iodoacetophenone (49 mg, 0.2 mmol) in 1:1 CH_2Cl_2/TFE (2 mL) was added *m*CPBA (49 mg, 0.2 mmol), followed with TsOH*H_2O (38 mg, 0.2 mmol). The resulting yellow solution was stirred at room temperature for 1 hour and then concentrated under a stream of air. Et_2O (4 mL) was added to the remaining residue and the resulting precipitate was filtered off to afford iodane **4** as an off-white solid (62 mg, 71%). Pure material was obtained after precipitation from a mixture of MeOH/CH_2Cl_2/hexanes. ^{1}H NMR (400 MHz, DMSO-d_6, ppm) δ 8.32- 8.29 (m, 2H), 8.11 – 8.09 (m, 2H), 7.49 – 7.47 (m, 2H), 7.13 –

7.11 (m, 2H), 2.63 (s, 3H), 2.28 (s, 3H). $^{13}C\{^{1}H\}$ NMR (100.6 MHz, DMSO-d_6, ppm) δ 197.5, 145.4, 139.2, 137.9, 134.4, 130.5, 128.2, 127.7, 125.6, 27.1, 20.9. Anal. Calcd for $C_{15}H_{15}IO_5S$: C, 41.49; H, 3.48. Found: C, 41.54; H, 3.49.

General Procedure A for the Synthesis of Imines 7a–q.[37] Benzaldehyde (2 mmol, 1.0 equiv.) was added to a mixture of *ortho*-aminophenol (2 mmol, 1.0 equiv), anhydrous Na_2SO_4 (3 equiv), and anhydrous CH_2Cl_2 (5 mL) under argon atmosphere. The suspension was stirred at room temperature for 16 h whereupon Na_2SO_4 was removed by filtration. The filtrate was concentrated under reduced pressure and the crude solid residue was recrystallized from EtOH to afford the corresponding imine.

General Procedure B for the Synthesis of Imines 7a–q.[37] A mixture of *ortho*-aminophenol (2 mmol, 1.0 equiv.) and aldehyde (2 mmol, 1.0 equiv.) was stirred under reflux in anhydrous EtOH (4 mL) for 4 hours. After cooling to room temperature and concentration under reduced pressure, the crude solid residue was recrystallized from EtOH to afford the corresponding imine.

General Procedure C for the Synthesis of Imines 7a–q.[38] A mixture of *ortho*-aminophenol (2 mmol, 1.0 equiv.) and aldehyde (2.4 mmol, 1.2 equiv.) was stirred at 70 °C in anhydrous MeOH (4 mL) in the presence of molecular sieves 4Å (1.5 g) for 20 hours. After being cooled to ambient temperature the reaction mixture was filtered to remove the molecular sieves, and the filtrate was concentrated under reduced pressure. The crude product was recrystallized from MeOH, EtOH or a mixture of MeOH/CH_2Cl_2/hexanes to yield the corresponding imine.

(*E*)-2-(Benzylideneamino)phenol (7a) was obtained as a light yellow amorphous solid (319 mg, 81%) according to general procedure A. ^{1}H-NMR spectral data are identical to those reported in the literature.[39] ^{1}H NMR (300 MHz, $CDCl_3$, ppm) δ 8.71 (s, 1H), 7.97 – 7.92 (m, 2H), 7.54 – 7.49 (m, 3H), 7.33 (dd, J = 7.9, 1.5 Hz, 1H), 7.29 (br s, 1H), 7.25 – 7.20 (m, 1H), 7.05 (dd, J = 8.1, 1.1 Hz, 1H), 6.96 – 6.91 (m, 1H). $^{13}C\{^{1}H\}$ NMR (75 MHz, $CDCl_3$, ppm) δ 157.1, 152.3, 135.8, 135.5, 131.7, 128.9, 128.8, 128.7, 120.1, 115.82, 115.0.

(*E*)-2-(4-Bromobenzylideneamino)phenol (7b) was obtained as a yellow solid (447 mg, 81%) according to general procedure A. Pure material was obtained by recrystallization from EtOH, mp 127–128 °C. IR

(film, cm^{-1}) 3312 (O–H), 1626 (C=N). ^1H NMR (400 MHz, CD_2Cl_2, ppm) δ 8.68 (s, 1H), 7.85 – 7.801 (m, 2H), 7.67 – 7.62 (m, 2H), 7.34 (dd, J = 8.0, 1.4 Hz, 1H), 7.26 – 7.15 (m, 2H), 6.99 (dd, J = 8.1, 1.4 Hz, 1H), 6.92 (td, J = 7.7, 1.4 Hz, 1H). $^{13}C\{^1H\}$NMR (100.6 MHz, $CDCl_3$, ppm) δ 155.7, 152.5, 135.2, 134.9, 132.3, 130.2, 129.4, 126.4, 120.3, 115.9, 115.3. HRMS (ESI-TOF) *m/z*: $[M+H]^+$ Calcd for $C_{13}H_{11}BrNO$ 276.0024; Found 276.0032.

(*E*)-2-(2-Nitrobenzylideneamino)phenol (7c) was obtained as a yellow solid (391 mg, 54%) according to general procedure B from *ortho*-aminophenol (3 mmol) and 2-nitrobenzaldehyde (3 mmol). ^1H-NMR spectral data are identical to those reported in the literature.[40] ^1H NMR (300 MHz, $CDCl_3$, ppm) δ 9.18 (s, 1H), 8.28 (dd, J = 7.7, 1.5 Hz, 1H), 8.08 (dd, J = 8.2, 1.2 Hz, 1H), 7.79 – 7.74 (m, 1H), 7.68 – 7.62 (m, 1H), 7.37 (dd, J = 7.9, 1.5 Hz, 1H), 7.30 – 7.24 (m, 1H), 7.15 (s, 1H), 7.05 (dd, J = 8.1, 1.3 Hz, 1H), 6.97 – 6.92 (m, 1H). $^{13}C\{^1H\}$ NMR (63 MHz, $CDCl_3$, ppm) δ 152.8, 152.0, 149.4, 134.7, 133.4, 131.4, 130.5, 130.2, 129.5, 124.7, 120.4, 116.4, 115.5.

(*E*)-2-((2,4,6-Trimethylbenzylidene)amino)phenol (7d) was obtained as a brown amorphous solid (84 mg, 70%) according to general procedure C from *ortho*-aminophenol (0.5 mmol) and 2,4,6-trimethylbenzaldehyde (0.5 mmol). ^1H-NMR spectral data are identical to those reported in the literature.[38] ^1H NMR (400 MHz, $CDCl_3$, ppm) δ 9.09 (s, 1H), 7.28 – 7.26 (m, 1H), 7.23 – 7.19 (m, 1H), 7.05 – 7.03 (m, 1H), 6.97 (s, 2H), 6.97 – 6.92 (m, 1H), 2.58 (s, 6H), 2.35 (s, 3H). $^{13}C\{^1H\}$ NMR (100.6 MHz, $CDCl_3$, ppm) δ 157.9, 152.2, 140.6, 139.2, 137.0, 130.3, 130.1, 128.7, 120.2, 115.6, 114.9, 21.7, 21.4.

(*E*)-2-(4-Methoxybenzylideneamino)phenol (7e) was obtained as a yellow amorphous solid (186 mg, 41%) according to general procedure A. ^1H NMR spectral data are identical to those reported in the literature.[41] ^1H NMR (300 MHz, $CDCl_3$, ppm) δ 8.63 (s, 1H), 7.91 – 7.86 (m, 2H), 7.30 – 7.27 (m, 1H), 7.21 – 7.15 (m, 1H), 7.03 – 6.99 (m, 3H), 6.94 – 6.88 (m, 1H), 3.90 (s, 3H). $^{13}C\{^1H\}$ NMR (63 MHz, $CDCl_3$, ppm) δ 162.5, 156.6, 152.0, 135.9, 130.6, 128.9, 128.3, 120.0, 115.7, 114.8, 114.3, 44.5.

(*E*)-2-((2-(Allyloxy)benzylidene)amino)phenol (7f) was obtained as a dark brown oil (493 mg, 99% yield) according to general procedure C. IR (film, cm^{-1}) 3412 (O–H), 1594 (C=N). ^1H NMR (400 MHz,

$CDCl_3$, ppm) δ 9.22 (s, 1H), 8.17 (dd, J = 7.7, 1.8 Hz, 1H), 7.44 (m, 1H), 7.32 (dd, J = 7.9, 1.5 Hz, 1H), 7.14 (td, J = 7.8, 1.5 Hz, 1H), 7.06 (t, J = 7.5 Hz, 1H), 7.02 (dd, J = 8.1, 1.4 Hz, 1H), 6.96 (d, J = 8.4 Hz, 1H), 6.91 (td, J = 7.7, 1.4 Hz, 1H), 6.16 – 6.06 (m, 1H), 5.46 (dd, J = 17.2, 1.6 Hz, 1H), 5.35 (dd, J = 10.5, 1.5 Hz, 1H), 4.66 (d, J = 5.2 Hz, 2H). $^{13}C\{^1H\}$ NMR (100.6 MHz, $CDCl_3$, ppm) δ 158.8, 153.3, 152.4, 136.4, 133.0, 132.9, 128.7, 127.6, 124.8, 121.2, 120.2, 118.1, 116.2, 114.9, 112.7, 69.4. HRMS (ESI-TOF) *m/z*: $[M+H]^+$ Calcd for $C_{16}H_{16}NO_2$ 254.1181; Found 254.1180.

(*E*)-2-((2-Allylbenzylidene)amino)phenol (7g) was obtained as a brown oil (260 mg, 90%) according to general procedure C from *ortho*-aminophenol (1.5 mmol) and 2-allylbenzaldehyde[42] (1.2 mmol). IR (film, cm^{-1}) 3412 (O – H), 1587 (C=N). ^1H NMR (400 MHz, $CDCl_3$, ppm) δ 8.96 (s, 1H), 8.12 (dd, J = 7.7, 1.5 Hz, 1H), 7.44 (td, J = 7.4, 1.5 Hz, 1H), 7.39 – 7.35 (m, 1H), 7.29 – 7.23 (m, 2H), 7.22 – 7.18 (m, 1H), 7.02 (dd, J = 8.1, 1.3 Hz, 1H), 6.93 – 6.89 (m, 1H), 6.08 (ddt, J = 17.1, 10.2, 5.8 Hz, 1H), 5.17 – 5.11 (m, 1H), 5.02 – 4.94 (m, 1H), 3.75 (d, J = 5.8 Hz, 2H). $^{13}C\{^1H\}$ NMR (100.6 MHz, $CDCl_3$, ppm) δ 156.0. 152.5, 1410.4, 137.3, 136.3, 133.9, 131.6, 131.0, 129.0, 128.5, 127.1. 120.2, 116.6, 116.0, 115.1, 37.4. HRMS (ESI-TOF) *m/z*: $[M+H]^+$ Calcd for $C_{16}H_{16}NO$ 238.1232; Found 238.1236.

(*E*)-2-((Pyridin-2-yl)methyleneamino)phenol (7h) was obtained as a green solid (282 mg, 47%) according to general procedure B from 2-pyridinecarboxaldehyde (3 mmol) and *ortho*-aminophenol (3 mmol). Pure material was obtained by recrystallization from hexanes/CH_2Cl_2, mp 104–105 ^oC. IR (film, cm^{-1}) 3362 (O–H), 1588 (HC=N). ^1H NMR (300 MHz, acetone-d_6, ppm) δ 8.82 (s, 1H), 8.70 (dd, J = 4.8, 0.8 Hz, 1H), 8.43 (d, J = 8.0 Hz, 1H), 7.91 (td, J = 7.5, 1.2 Hz, 1H), 7.49 – 7.45 (m, 2H), 7.28 – 7.4 (m, 1H), 6.98 – 6.89 (m, 2H). $^{13}C\{^1H\}$ NMR (100.6 MHz, acetone-d_6, ppm) δ 159.3, 155.7, 153.7, 150.5, 137.4, 136.6, 130.1, 126.1, 122.4, 120.8, 118.2, 116.6. HRMS (ESI-TOF) *m/z*: $[M+H]^+$ Calcd for $C_{12}H_{11}N_2O$ 198.0788; Found 198.0782.

(2*E*)-2-((*E*)-3-Phenylallylideneamino)phenol (7i) was obtained as a light yellow solid (112 mg, 25%) according to general procedure A. ^1H-NMR spectral data are identical to those reported in the literature.[43] ^1H NMR (300 MHz, $CDCl_3$, ppm) δ 8.51 (d, J = 7.7 Hz, 1H), 7.59 – 7.55 (m, 2H), 7.47 – 7.38 (m, 3H),

7.27 – 7.16 (m, 4H), 7.01 (dd, J = 8.1, 1.1 Hz, 1H), 6.92 – 6.87 (m, 1H). $^{13}C\{^1H\}$ NMR (63 MHz, $CDCl_3$, ppm) δ 158.2, 152.3, 144.2, 135.6, 135.5, 129.8, 129.0, 128.9, 128.5, 127.6, 120.0, 115.5, 115.0.

(*E*)-2-(Benzylideneamino)-5-methylphenol (7k) was obtained as a yellow solid (413 mg, 98%) according to general procedure B. Pure material was obtained by recrystallization from EtOH, mp 94–96 °C. IR (film, cm^{-1}) 3332 (O–H), 1580 (C=N). ^1H NMR (300 MHz, $CDCl_3$, ppm) δ 8.70 (s, 1H), 7.94 – 7.90 (m, 2H), 7.52 – 7.47 (m, 3H), 7.28 (br s, 1H), 7.24 (d, J = 8.1 Hz, 1H), 6.86 (m, 1H), 6.75 – 6.72 (m, 1H), 2.35 (s, 3H). $^{13}C\{^1H\}$ NMR (75 MHz, $CDCl_3$, ppm) δ 155.7, 152.3, 139.4, 136.0, 132.9, 131.4, 128.8, 128.6, 120.8, 115.5, 115.4, 21.5. HRMS (ESI-TOF) *m/z*: $[M]^+$ Calcd for $C_{14}H_{13}NO$ 211.0992; Found 211.0984.

(*E*)-2-(Benzylideneamino)-4-methylphenol (7l) was obtained as a light yellow amorphous solid (17 mg, 4%) according to general procedure B. ^1H-NMR spectral data are identical to those reported in the literature.[44] ^1H NMR (300 MHz, $CDCl_3$ ppm) δ 8.70 (s, 1H), 7.95 – 7.91 (m, 2H), 7.53 – 7.48 (m, 3H), 7.14 – 7.13 (m, 1H), 7.09 (br s, 1H), 7.05 – 7.01 (m, 1H), 6.94 – 6.91 (m, 1H), 2.34 (s, 3H). $^{13}C\{^1H\}$ NMR (63 MHz, $CDCl_3$, ppm) δ 156.7, 150.1, 135.9, 135.1, 131.6, 129.5, 128.8, 128.7, 116.3, 114.6, 20.8.

(*E*)-2-(Benzylideneamino)-5-nitrophenol (7m) was obtained as a yellow amorphous solid (353 mg, 55%) according to general procedure C. The pure product was obtained after precipitating from a mixture of MeOH/DCM/hexanes. ^1H NMR (400 MHz, acetone-d_6, ppm) δ 8.88 (s, 1H), 8.11 – 8.08 (m, 2H), 7.80 (dd, J = 8.7, 2.5 Hz, 1H), 7.75 (d, J = 2.5 Hz, 1H), 7.62 – 7.53 (m, 3H), 7.49 (d, J = 8.6 Hz, 1H). $^{13}C\{^1H\}$ NMR (100.6 MHz, acetone-d_6, ppm) δ 163.9, 152.9, 147.7, 144.8, 136.8, 133.2, 130.5, 129.7, 119.5, 116.2, 111.3. HRMS (ESI-TOF) *m/z*: $[M+H]^+$ Calcd for $C_{13}H_{11}N_2O_3$ 243.0770; Found 243.0765.

(*E*)-Methyl 4-(3,5-dichlorobenzylideneamino)-3-hydroxybenzoate (7n) was obtained as a yellow solid (486 mg, 75%) according to general procedure A. Pure material was obtained by recrystallization from EtOH, mp 207 – 208 °C. IR (film, cm^{-1}) 3394 (O–H), 1714 (C=O), 1562 (C=N). ^1H NMR (300 MHz, DMSO, ppm) δ 8.73 (s, 1H), 8.09 (d, J = 2.1 Hz, 2H), 7.79 (t, J = 2.0 Hz, 1H), 7.47 (s, 1H), 7.46 (dd, J = 6.0, 1.9 Hz, 1H), 7.29 – 7.26 (m, 1H), 3.83 (s, 3H). $^{13}C\{^1H\}$ NMR (63 MHz, DMSO, ppm) δ 165.9,

158.9, 151.0, 141.5, 139.3, 134.6, 130.7, 128.7, 127.4, 120.6, 119.7, 116.8, 52.1. HRMS (ESI-TOF) *m/z*: $[M+H]^+$ Calcd for $C_{15}H_{12}Cl_2NO_3$ 324.0194; Found 324.0190.

(*E*)-2-((4-Bromobenzylidene)amino)-4-nitrophenol (7o) was obtained as a yellow amorphous solid (238 mg, 37%) according to general procedure C. Pure product was obtained after precipitating from a mixture of MeOH/DCM. ^{1}H NMR (400 MHz, $CDCl_3$, ppm) δ 8.69 (s, 1H), 7.86 – 7.81 (m, 4H), 7.67 (d, J = 8.4 Hz, 2H), 7.34 (d, J = 8.7 Hz, 1H), 7.17 (s, 1H). $^{13}C\{^1H\}$ NMR (100.6 MHz, $CDCl_3$, ppm) δ 160.4, 152.2, 147.7, 141.2, 134.0, 132.6, 130.8, 128.0, 116.6, 116.1, 110.8. HRMS (ESI-TOF) *m/z*: $[M+H]^+$ Calcd for $C_{13}H_{10}BrN_2O_3$ 320.9875; Found 320.9867.

(*E*)-4-Nitro-2-((3,4,5-trimethoxybenzylidene)amino)phenol (7p) was obtained as a yellow solid (215 mg, 72%) according to general procedure C from 2-amino-4-nitrophenol (0.9 mmol) and 3,4,5-trimethoxybenzaldehyde (0.9 mmol). Pure material was obtained by recrystallization from CH_2Cl_2, mp 187–188 ^oC. IR (film, cm^{-1}) 3349 (O–H), 1581 (C=N), 1462 (NO_2). ^{1}H NMR (400 MHz, $CDCl_3$, ppm) δ 8.70 (s, 1H), 8.22 (d, J = 2.6 Hz, 1H), 8.14 (dd, J = 9.0, 2.6 Hz, 1H), 7.19 (s, 2H), 7.10 (d, J = 8.9 Hz, 1H), 3.97 (s, 6H), 3.96 (s, 3H). $^{13}C\{^1H\}$ NMR (100.6 MHz, $CDCl_3$, ppm) δ 160.4, 157.7, 153.8, 142.5, 141.4, 135.9, 130.3, 124.5, 115.1, 112.3, 106.6, 61.2, 56.5. HRMS (ESI-TOF) *m/z*: $[M+H]^+$ Calcd for $C_{16}H_{17}N_2O_6$ 333.1087; Found 333.1091.

3-(3-Amino-4-hydroxyphenyl)propanoic acid (14). To a solution of 3-(4-hydroxy-3-nitrophenyl)propanoic acid (815 mg, 3.86 mmol) in abs. EtOH (50 mL) was added 10% Pd–C (402 mg, 10 mol %). and H_2 gas was passed through the resulting suspension at room temperature for 2 hours. Progress of the hydrogenation was followed by UPLC-MS analysis. Once the reaction is completed, it was filtered through a plug of Celite. The filtrate was concentrated to obtain the product as pale green foam (636 mg, 91%) that was used in the next step without additional purification. IR (film, cm^{-1}) 3370, 3335 (N–H), 2934 (O–H). ^{1}H NMR (400 MHz, CD_3OD, ppm) δ 6.64 (d, J = 2.2 Hz, 1H), 6.61 (d, J = 8.0 Hz, 1H), 6.47 (dd, J = 8.0, 2.2 Hz, 1H), 2.74 (t, J = 7.8 Hz, 2H), 2.50 (t, J = 7.8 Hz, 1H). $^{13}C\{^1H\}$ NMR (100.6 MHz, CD_3OD, ppm) δ 177.6, 145.0, 135.4, 133.8, 120.2, 117.7, 115.6, 37.6, 31.7. HRMS(ESI-TOF) *m/z*: $[M+H]^+$ Calcd for $C_9H_{12}NO_3$ 182.0817; Found 182.0817.

(*E*)-3-(3-((4-Bromobenzylidene)amino)-4-hydroxyphenyl)propanoic acid (7q) was obtained as a brown amorphous solid (106 mg, 25%) according to general procedure C from 3-(3-amino-4-hydroxyphenyl)propanoic acid (**14**; see above) (1.2 mmol) and 4-bromobenzaldehyde (1.5 mmol); product **7q** was used in the next step without additional purification because of its instability. IR (film, cm^{-1}) 3409 (O–H), 1699 (C=O), 1586 (C=N). ^{1}H NMR (300 MHz, CD_3OD, ppm) δ 8.67 (s, 1H), 7.92 – 7.89 (m, 2H), 7.65 – 7.63 (m, 2H), 7.13 (d, J = 2.1 Hz, 1H), 7.01 (dd, J = 8.2, 1.9 Hz, 1H), 6.81 (d, J = 8.2 Hz, 1H), 2.86 (t, J = 7.7 Hz, 2H), 2.52 (t, J = 7.7 Hz, 2H). ^{13}C{^{1}H} NMR (100.6 MHz, CD_3OD, ppm) δ 176.9, 159.2, 151.2, 138.3, 136.9, 133.9, 133.0, 131.5, 129.1, 126.6, 119.1, 116.7, 37.1, 31.4. HRMS (ESI-TOF) *m/z*: $[M+H]^+$ Calcd for $C_{16}H_{15}BrNO_3$ 348.0235; Found 348.0237

General Procedure D for the Synthesis of Substituted Benzoxazoles from Imines. A solution of electrochemically prepared I(III) oxidant **2** (67 mM in HFIP) was added under argon to a solution of imine (0.3 mmol) in HFIP (0.5 mL). The resulting solution was stirred at room temperature until complete conversion of **7** (usually 10 min) and the progress of the reaction was monitored by GC-MS and ^{1}H NMR. Diethylether (50 mL) was then added and the resulting suspension was kept at +4 °C for 15 minutes. The formed precipitate (iodoarene **1**) was removed by filtration and washed with Et_2O. Drying under air allowed for 92-94% recovery of mediator **1**. The combined filtrates were concentrated under reduced pressure and the residue was purified by column chromatography on silica gel to yield the corresponding substituted benzoxazole.

General Procedure E for One-pot Two-step Synthesis of Substituted Benzoxazoles from the Aldehyde and Aniline. A light brown solution of *ortho*-aminophenol (0.4 mmol, 1 equiv) and aldehyde (0.48 mmol, 1.2 equiv) in $CHCl_3$ (2 mL; for benzoxazole **8j**) or in HFIP (2mL; for benzoxazole **8b**) was stirred at room temperature for 6 hours. Then freshly prepared I(III) reagent **2** (67 mM solution in HFIP) was added under argon atmosphere and stirring at room temperature was continued for 30 minutes. Addition of diethylether (50 mL) afforded a suspension that was cooled at +4 °C for 15 minutes. The formed sand-colored precipitate (iodoarene **1**) was removed by filtration. The filter cake was washed with

Et_2O and dried under air. The filtrate was concentrated and the residue was purified by column chromatography on silica gel to yield the corresponding benzoxazole.

2-Phenylbenzo[*d*]oxazole (8a) was obtained as a white solid (51 mg, 87%) according to general procedure D. The crude product was purified by column chromatography on silica gel using gradient elution from 0% EtOAc in heptane to 9% EtOAc in heptane. Analytical TLC on silica gel, 1:9 EtOAc/heptane, R_f = 0.4. Pure material was obtained by recrystallization from heptane, mp 105.5 – 106.5 °C. ^{1}H-NMR spectral data are identical to those reported in the literature.[37] ^{1}H NMR (300 MHz, $CDCl_3$, ppm) δ 8.31 – 8.25 (m, 2H), 7.82 – 7.77 (m, 1H), 7.62 – 7.58 (m, 1H), 7.57 – 7.52 (m, 3H), 7.40 – 7.34 (m, 2H). ^{13}C{^{1}H} NMR (75 MHz, $CDCl_3$, ppm) δ 163.0, 150.7, 142.1, 131.5, 128.9, 127.6, 127.1, 125.1, 124.5, 120.0, 110.5. GC-MS (EI) *m/z*: $[M]^+$ found for $C_{13}H_9NO$ 195.38.

2-(4-Bromophenyl)benzo[*d*]oxazole (8b) was obtained as a white solid (71 mg, 87%) according to general procedure D. The crude product was purified by column chromatography on silica gel using gradient elution from 0% EtOAc in heptane to 9% EtOAc in heptane. Analytical TLC on silica gel, 1:9 EtOAc/heptane, R_f = 0.45. Pure material was obtained by recrystallization from heptane, mp 158.5 – 159.5 °C. ^{1}H-NMR spectral data are identical to those reported in literature.[37] ^{1}H NMR (300 MHz, $CDCl_3$, ppm) δ 8.14 – 8.10 (m, 2H), 7.80 – 7.74 (m, 1H), 7.69 – 7.64 (m, 2H), 7.61 – 7.55 (m, 1H), 7.40 – 7.34 (m, 2H). ^{13}C{^{1}H} NMR (63 MHz, $CDCl_3$, ppm) δ 162.1, 150.7, 142.0, 132.2, 129.0, 126.2, 126.1, 125.4, 124.8, 120.1, 110.6. GC-MS (EI) *m/z*: $[M]^+$ found for $C_{13}H_8BrNO$ 273.44.

Use of general procedure E afforded benzoxazole **8b** in 81% yield (66 mg).

2-(2-Nitrophenyl)benzo[*d*]oxazole (8c) was obtained as pale yellow solid (64 mg, 89%) according to general procedure D. The crude product was purified by column chromatography on silica gel using gradient elution from 0% EtOAc in heptane to 33% EtOAc in heptane. Analytical TLC on silica gel, 1:9 EtOAc/heptane, R_f = 0.1. Pure material was obtained by recrystallization from heptane, mp 104.5 – 105.5 °C. ^{1}H-NMR spectral data are identical to those reported in literature.[45] ^{1}H NMR (300 MHz, $CDCl_3$, ppm) δ 8.17 – 8.14 (m, 1H), 7.92 – 7.89 (dd, J = 7.9, 1.5 Hz, 1H), 7.85 – 7.79 (m, 1H), 7.78 – 7.67 (m, 2H), 7.62 – 7.55 (m, 1H), 7.45 – 7.37 (m, 2H). ^{13}C{^{1}H} NMR (75 MHz, $CDCl_3$, ppm) δ 158.8, 151.0, 141.5,

132.3, 131.8, 131.4, 126.0, 124.9, 124.2, 121.5, 120.7, 110.9. GC-MS (EI) *m/z*: $[M]^+$ found for $C_{13}H_8N_2O_3$ 240.38.

2-Mesitylbenzo[*d*]oxazole (8d) was obtained as a yellow thick oil (56 mg, 79%) according to general procedure D. The crude product was purified by column chromatography on silica gel using gradient elution from 3% EtOAc in hexanes to 15% EtOAC in hexanes. Analytical TLC on silica gel, 1:10 EtOAc/hexanes, R_f = 0.48. ^{1}H-NMR spectral data are identical to those reported in literature.[37] ^{1}H NMR (400 MHz, $CDCl_3$, ppm) δ 7.86 – 7.79 (m, 1H), 7.62 – 7.56 (m, 1H), 7.41–7.35 (m, 2H), 6.98 (s, 2H), 2.36 (s, 3H), 2.29 (s, 6H). $^{13}C\{^1H\}$ NMR (100.6 MHz, $CDCl_3$, ppm) δ 163.4, 150.8, 141.7, 140.4, 138.6, 128.8, 125.1, 125.0, 124.3, 120.3, 110.7, 21.4, 20.5. UPLC-MS (ESI) *m/z*: $[M+H]^+$ found for $C_{16}H_{16}NO$ 238.29.

2-(4-Methoxyphenyl)benzo[*d*]oxazole (8e) was obtained as light brown solid (51 mg, 75%) according to general procedure D. The crude product was purified by column chromatography on silica gel using gradient elution from 0% EtOAc in heptane to 33% EtOAc in heptane. Analytical TLC on silica gel, 1:9 EtOAc/heptane, R_f = 0.2. Pure material was obtained by recrystallization from heptane, mp 99–100 ^{o}C. ^{1}H-NMR spectral data are identical to those reported in literature.[37] ^{1}H NMR (300 MHz, $CDCl_3$, ppm) δ 8.23 – 8.18 (m, 2H), 7.78 – 7.72 (m, 1H), 7.59 – 7.53 (m, 1H), 7.37 – 7.29 (m, 2H), 7.06 – 7.01 (m, 2H), 3.90 (s, 3H). $^{13}C\{^1H\}$ NMR (63 MHz, $CDCl_3$, ppm) δ 163.2, 162.3, 150.7, 142.3, 129.4, 124.6, 124.4, 119.7, 119.6, 114.3, 110.4, 55.4. GC-MS (EI) *m/z*: $[M]^+$ found for $C_{14}H_{11}NO_2$ 225.44.

2-(2-(Allyloxy)phenyl)benzo[*d*]oxazole (8f) was obtained as a light orange amorphous solid (33 mg, 46%) according to general procedure D. The crude product was purified by column chromatography on silica gel using gradient elution from 3% EtOAc in hexanes to 10% EtOAc in hexanes. Analytical TLC on silica gel, 1:4 EtOAc/hexanes, R_f = 0.55. ^{1}H NMR (400 MHz, $CDCl_3$, ppm) δ 8.15 (dd, J = 7.7, 1.8 Hz, 1H), 7.83 – 7.79 (m, 1H), 7.61 – 7.57 (m, 1H), 7.48 – 7.44 (m,1H), 7.40 – 7.30 (m, 2H), 7.11 – 7.03 (m, 2H), 6.15 – 6.06 (m, 1H), 5.64 (dq, J = 17.3, 1.8 Hz, 1H), 5.33 (dq, J = 10.7, 1.6 Hz, 1H), 4.75 (dt, J = 4.7, 1.8 Hz, 2H). $^{13}C\{^1H\}$ NMR (100.6 MHz, $CDCl_3$, ppm) δ 162.1, 157.6, 150.7, 142.1, 132.9, 132.7,

131.6, 125.0, 124.4, 121.1, 120.2, 117.4, 116.9, 113.8, 110.6, 69.7. HRMS (ESI-TOF) *m/z*: $[M+H]^+$ Calcd for $C_{16}H_{14}NO_2$ 252.1025; Found 252.1029.

2-(2-Allylphenyl)benzo[*d*]oxazole (8g) was obtained as a light yellow oil (28 mg, 40%) according to general procedure D. The crude product was purified by column chromatography on silica gel using isocratic elution with 2% EtOAc in hexanes. Analytical TLC on silica gel, 1:10 EtOAc/hexanes, R_f = 0.58. ^{1}H NMR (400 MHz, $CDCl_3$, ppm) δ 8.18 – 8.15 (m, 1H), 7.83 – 7.79 (m, 1H), 7.62 – 7.58 (m, 1H), 7.49 – 7.45 (m, 1H), 7.41 – 7.35 (m, 4H), 6.14 – 6.04 (m, 1H), 5.11 – 5.04 (m, 2H), 4.05 (d, J = 6.6 Hz, 1H). $^{13}C\{^1H\}$ NMR (100.6 MHz, $CDCl_3$, ppm) δ 163.1, 150.5, 142.2, 140.8, 137.3, 131.2, 131.1, 130.4, 126.6, 126.2, 125.2, 124.5, 120.3, 116.0, 110.6, 38.6. HRMS (ESI-TOF) *m/z*: $[M+H]^+$ Calcd for $C_{16}H_{14}NO$ 236.1075; Found 236.1074.

2-(Pyridin-2-yl)benzo[*d*]oxazole (8h) was obtained as an off-white solid (56 mg, 95%) according to general procedure D. The crude product was purified by column chromatography on silica gel using gradient elution from 0% EtOAc in heptane to 33% EtOAc in heptane. Analytical TLC on silica gel, 1:4 EtOAc/ heptane, R_f=0.15. Pure material was obtained by recrystallization from heptane, mp 100.5 – 101.5 ^{o}C. ^{1}H-NMR spectral data are identical to those reported in the literature.[46] ^{1}H NMR (300 MHz, $CDCl_3$, ppm) δ 9.41 (br s, 1H), 8.71 (d, J = 4.3 Hz, 1H), 8.54 – 8.51 (m, 1H), 7.80 – 7.77 (m, 1H), 7.61 – 7.56 (m, 1H), 7.48 (dd, J = 7.8, 5.0 Hz, 1H), 7.42 – 7.35 (m, 2H). $^{13}C\{^1H\}$ NMR (63 MHz, $CDCl_3$, ppm) δ 160.3, 151.2, 150.7, 147.9, 141.5, 135.3, 125.8, 125.0, 123.9, 123.8, 120.3, 110.8. GC-MS (EI) *m/z*: $[M]^+$ found for $C_{12}H_8N_2O$ 196.41.

(*E*)-2-Styrylbenzo[*d*]oxazole (8i) was obtained as a pale yellow solid (52 mg, 78%) according to general procedure D. The crude product was purified by column chromatography on silica gel using gradient elution from 0% EtOAc in heptane to 9% EtOAc in heptane. Analytical TLC on silica gel, 1:9 EtOAc/ heptane, R_f = 0.23. Pure material was obtained by recrystallization from heptane, mp 83.5 – 84.5 ^{o}C. ^{1}H-NMR spectral data are identical to those reported in the literature.[47] ^{1}H NMR (300 MHz, $CDCl_3$, ppm) δ 7.81 (d, J = 16.4 Hz, 1H), 7.76 – 7.71 (m, 1H), 7.63 – 7.59 (m, 2H), 7.57 – 7.51 (m, 1H), 7.47 – 7.39 (m, 3H), 7.38 – 7.32 (m, 2H), 7.10 (d, J = 16.4 Hz, 1H). $^{13}C\{^1H\}$ NMR (75 MHz, $CDCl_3$, ppm) δ 162.8,

150.4, 142.2, 139.5, 135.1, 129.8, 129.0, 127.6, 125.2, 124.5, 119.9, 113.9, 110.3. GC-MS (EI) *m/z*: $[M]^+$ found for $C_{15}H_{11}NO$ 221.45.

2-*Tert*-butylbenzo[*d*]oxazole (8j) was obtained as an off-white amorphous solid (52 mg, 74%) according to general procedure E. The crude product was purified by column chromatography on silica gel using gradient elution from 0% EtOAc in heptane to 33% EtOAc in heptane. Analytical TLC on silica gel, 1:9 EtOAc/heptane, R_f = 0.33. ^{1}H-NMR spectral data are identical to those reported in the literature.[39] ^{1}H NMR (300 MHz, $CDCl_3$, ppm) δ 7.73 – 7.68 (m, 1H), 7.50 – 7.46 (m, 1H), 7.32 – 7.26 (m, 2H), 1.50 (s, 9H). $^{13}C\{^1H\}$ NMR (63 MHz, $CDCl_3$, ppm) δ 173.5, 150.8, 141.2, 124.3, 123.9, 119.7, 110.3, 34.1, 28.4. GC-MS (EI) *m/z*: $[M]^+$ found for $C_{11}H_{13}NO$ 175.32.

6-Methyl-2-phenylbenzo[*d*]oxazole (8k) was obtained as an off-white solid (47 mg, 75%) according to general procedure D. The crude product was purified by column chromatography on silica gel using gradient elution from 0% EtOAc in heptane to 10% EtOAc in heptane. Analytical TLC on silica gel, 1:9 EtOAc/heptane, R_f = 0.35. Pure material was obtained by recrystallization from heptane, mp 92 – 93 °C. ^{1}H-NMR spectral data are identical to those reported in the literature.[48] ^{1}H NMR (300 MHz, $CDCl_3$, ppm) δ 8.27 – 8.23 (m, 2H), 7.65 (d, J = 8.1 Hz, 1H), 7.55 – 7.50 (m, 3H), 7.39 (dt, J = 1.6, 0.6 Hz, 1H), 7.19 – 7.16 (m, 1H), 2.52 (s, 3H). $^{13}C\{^1H\}$ NMR (75 MHz, $CDCl_3$, ppm) δ 162.5, 151.0, 139.9, 135.5, 131.2, 128.8, 127.4, 127.3, 125.8, 119.3, 110.7, 21.8. GC-MS (EI) *m/z*: $[M]^+$ found for $C_{14}H_{11}NO$ 209.43.

5-Methyl-2-phenylbenzo[*d*]oxazole (8l) was obtained as an off-white amorphous solid (54 mg, 86%) according to general procedure D. The crude product was purified by column chromatography on silica gel using gradient elution from 0% EtOAc in heptane to 10% EtOAc in heptane. Analytical TLC on silica gel, 1:9 EtOAc/heptane, R_f = 0.36. ^{1}H-NMR spectral data are identical to those reported in the literature.[37] ^{1}H NMR (300 MHz, $CDCl_3$, ppm) δ 8.29 – 8.24 (m, 2H), 7.57(dt, J = 1.7, 0.8 Hz, 1H), 7.56 – 7.51 (m, 3H), 7.48 – 7.45 (d, J = 7.9 Hz, 1H), 7.19 – 7.15 (m, 1H), 2.50 (s, 3H). $^{13}C\{^1H\}$ NMR (75 MHz, $CDCl_3$, ppm) δ 163.1, 149.0, 142.3, 134.4, 131.4, 128.9, 127.5, 127.33, 126.2, 119.9, 109.9, 21.5. GC-MS (EI) *m/z*: $[M]^+$ found for $C_{14}H_{11}NO$ 209.44.

6-Nitro-2-phenylbenzo[*d*]oxazole (8m) was obtained as a light yellow amorphous solid (44 mg, 61%) according to general procedure D. The crude product was purified by column chromatography on silica gel using gradient elution from 0% EtOAc in heptane to 33% EtOAc in heptane; analytical TLC on silica gel, 1:9 EtOAc/heptane, R_f = 0.19. ^{1}H-NMR spectral data are identical to those reported in literature.[48] ^{1}H NMR (300 MHz, $(CD_3)_2O$, ppm) δ 8.62 (dd, J = 2.2, 0.5 Hz, 1H), 8.37 (dd, J = 8.8, 2.2 Hz, 1H), 8.34 – 8.31 (m, 2H), 7.98 (dd, J = 8.8, 0.5 Hz, 1H), 7.72 – 7.64 (m, 3H). ^{13}C{^{1}H} NMR (63 MHz, $CDCl_3$, ppm) δ 167.4, 149.9, 147.4, 145.1, 132.9, 129.2, 128.3, 126.0, 120.9, 119.8, 107.2. GC-MS (EI) *m/z*: $[M]^+$ found for $C_{13}H_8N_2O$ 240.43.

Methyl 2-(3,5-dichlorophenyl)benzo[*d*]oxazole-6-carboxylate (8n) was obtained as a white solid (87 mg, 90%) according to general procedure D. The crude product was purified by column chromatography on silica gel using gradient elution from 0% EtOAc in heptane to 10% EtOAc in heptane. Analytical TLC on silica gel, 1:9 EtOAc/heptane, R_f = 0.35. Pure material was obtained by recrystallization from heptane, mp 171.5 – 172.5 ^{o}C. IR (film, cm^{-1}) 1725 (C=O). ^{1}H NMR (250 MHz, $CDCl_3$, ppm) δ 8.27 (dd, J = 1.6, 0.6 Hz, 1H), 8.15 (d, J = 1.9 Hz, 2H), 8.12 (dd, J = 8.4, 1.6 Hz, 1H), 7.80 (dd, J = 8.5, 9.6 Hz, 1H), 7.54 (t, J = 1.9 Hz, 1H), 3.98 (s, 3H). ^{13}C{^{1}H} NMR (75 MHz, $CDCl_3$, ppm) δ 166.4, 162.8, 150.5, 145.5, 135.9, 131.9, 129.3, 127.9, 126.7, 126.1, 120.0, 113.5, 52.5. HRMS (ESI-TOF) *m/z*: $[M+H]^+$ Calcd for $C_{15}H_{10}Cl_2NO_3$ 322.0037; Found 322.0035.

2-(4-Bromophenyl)-5-nitrobenzo[*d*]oxazole (8o) was obtained as a sand-colored solid (62 mg, 69%) according to general procedure D. The crude product was purified by column chromatography on silica gel using gradient elution from 3% EtOAc in hexanes to 10% EtOAc in hexanes. Analytical TLC on silica gel, 1:10 EtOAc/hexanes, R_f = 0.44. Pure material was obtained by recrystallization from hexanes/CH_2Cl_2, mp 176-177 ^{o}C. ^{1}H-NMR spectral data are identical to those reported in the literature.[49] ^{1}H NMR (400 MHz, $CDCl_3$, ppm) δ 8.48 (dd, J = 2.2, 0.5 Hz, 1H), 8.32 (dd, J = 8.7, 2.2 Hz, 1H), 8.15 – 8.12 (m, 2H), 7.84 (dd, J = 8.7, 0.5 Hz, 1H), 7.72 – 7.69 (m, 2H). ^{13}C{^{1}H} NMR (100.6 MHz, $CDCl_3$, ppm) δ 166.6, 150.1, 147.4, 145.4, 132.7, 129.7, 128.0, 125.0, 121.1, 120.1, 107.4. HRMS (ESI-TOF) *m/z*: $[M+H]^+$ Calcd for $C_{13}H_8BrN_2O_3$ 318.9718; Found 318.9715.

5-Nitro-2-(3,4,5-trimethoxyphenyl)benzo[*d*]oxazole (8p) was obtained as a pale yellow solid (78 mg, 93%) according to general procedure D from (*E*)-4-nitro-2-((3,4,5-trimethoxybenzylidene)amino)phenol (**7p**) (84 mg, 0.25 mmol). Crude **8p** was purified by column chromatography on silica gel using gradient elution from 9% EtOAc in hexanes to 20% EtOAc in hexanes. Analytical TLC on silica gel, 1:4 EtOAc/hexanes, R_f = 0.28. Pure material was obtained by recrystallization for hexanes/CH_2Cl_2, mp 187 – 188 ^oC. IR (film, cm^{-1}) 1498 (NO_2). ^1H NMR (400 MHz, $CDCl_3$, ppm) δ 8.62 (d, J = 2.3 Hz, 1H), 8.32 (dd, J = 8.9, 2.4 Hz, 1H), 7.67 (d, J = 8.9 Hz, 1H), 7.51 (s, 2H), 4.00 (s, 6H), 3.96 (s, 3H). $^{13}C\{^1H\}$ NMR (100.6 MHz, $CDCl_3$, ppm) δ 166.0, 154.4, 153.8, 145.6, 142.8, 142.2, 121.2, 121.0, 116.2, 110.7, 105.4, 61.2, 56.6. HRMS (ESI-TOF) *m/z*: $[M+H]^+$ Calcd for $C_{16}H_{15}N_2O_6$ 331.0930; Found 331.0937.

3-(2-(4-Bromophenyl)benzo[*d*]oxazol-5-yl)propanoic acid (8q) was obtained as an amorphous sand-colored solid (37 mg, 91%) according to general procedure D from (*E*)-3-(3-((4-bromobenzylidene)amino)-4-hydroxyphenyl)propanoic acid (**7q**) (90 mg, 0.1 mmol). Crude **8q** was purified by column chromatography on silica gel using gradient elution from 3% MeOH in CH_2Cl_2 to 15% MeOH in CH_2Cl_2. Analytical TLC on silica gel, 1:40 MeOH/CH_2Cl_2, R_f = 0.26. IR (film, cm^{-1}) 3410 (O–H), 1700 (C=O). ^1H NMR (400 MHz, CD_3OD, ppm) δ 8.14 – 8.11 (m, 2H), 7.77 – 7.74 (m, 2H), 7.62 (d, J = 1.6 Hz, 1H), 7.58 (d, J = 8.5 Hz,1H), 7.33 (dd, J = 8.4, 1.7 Hz, 1H), 3.07 (t, J = 7.5 Hz, 2H), 2.66 (t, J = 7.6 Hz, 1H). $^{13}C\{^1H\}$ NMR (100.6 MHz, CD_3OD, ppm) δ 163.9, 150.7, 143.0, 139.7, 133.5, 130.1, 127.5, 127.4, 127.2, 120.2, 111.5, 111.4, 32.0, 29.5. HRMS (ESI-TOF) *m/z*: $[M+H]^+$ Calcd for $C_{16}H_{13}BrNO_3$ 346.0079; Found 346.0087.

1-Oxaspiro[4.5]deca-6,9-diene-2,8-dione (10) was obtained as light yellow amorphous solid (37 mg, 58%) according to general procedure D from 3-(4-hydroxyphenyl)propanoic acid (65 mg, 0.35 mmol). Crude **10** was purified by column chromatography on silica gel using gradient elution from 20% EtOAc in hexanes to 33% EtOAc in hexanes. ^1H-NMR spectral data are identical to those reported in the literature.[50] ^1H NMR (400 MHz, $CDCl_3$, ppm) δ 6.87 – 6.83 (m, 2H), 6.29 – 6.25 (m, 2H), 2.77 (t, J = 8.3 Hz, 2H), 2.37 (t, J = 8.3 Hz, 2H). $^{13}C\{^1H\}$ NMR (100.6 MHz, $CDCl_3$, ppm) δ 184.2, 175.2, 145.7, 129.3, 78.5, 32.4, 28.1.

6-Bromo-2-phenyl-2-(trifluoromethyl)-2,3-dihydrobenzo[*d*]oxazole (15). A mixture of 2-amino-5-bromophenol (950 mg, 5 mmol) and neat trifluoroacetophenone (1.54 mL, 11 mmol, 2 equiv) were stirred at 140 ^{o}C for 18 hours under argon atmosphere. The dark brown reaction solution was cooled to room temperature whereupon a dark solid was formed. The crude reaction mixture was dissolved in CH_2Cl_2 and purified by column chromatography on silica gel using isocratic elution with 4% EtOAc in hexanes as a mobile phase. The fractions containing product were combined and concentrated. The residue was repeatedly purified by reverse phase chromatography using gradient elution from 10% MeCN in water to 100% MeCN to afford **15** as a sand-colored amorphous solid (1.29 g, 68%); analytical TLC on silica gel, 1:10 EtOAc/hexanes, R_f = 0.26. IR (film, cm^{-1}) 3356 (N – H). ^{1}H NMR (400 MHz, $CDCl_3$, ppm) δ 7.68 – 7.68 (m, 2H), 7.51 – 7.47 (m, 3H), 7.08 (d, J = 1.8 Hz, 1H), 6.99 (dd, J = 8.1, 1.8 Hz, 1H), 6.70 (d, J = 8.1 Hz, 1H), 4.38 (s, 1H). ^{13}C{^{1}H} NMR (100.6 MHz, $CDCl_3$, ppm) δ 151.4, 135.2, 134.7, 130.4, 129.1, 125.8, 125.0, 122.83 (q, J = 287.7 Hz), 114.7, 113.5, 112.5, 98.8 (q, J = 32.6 Hz). ^{19}F NMR (376.3 MHz, $CDCl_3$) δ -83.87. HRMS (ESI-TOF) *m/z*: $[M+H]^+$ Calcd for $C_{14}H_{10}BrF_3NO$ 343.9898; Found 343.9886.

Benzyl (*E*)-3-(2-phenyl-2-(trifluoromethyl)-2,3-dihydrobenzo[*d*]oxazol-6-yl)acrylate (16) A vial (5 mL) was flushed with argon and charged with 6-bromo-2-phenyl-2-(trifluoromethyl)-2,3-dihydrobenzo[*d*]oxazole (**15**) (200 mg, 0.58 mg), $Pd(OAc)_2$ (13 mg, 10 mol %), and DMF (0.87 mL). Then, benzyl acrylate (178 µL, 1.16 mmol) was added, followed by triethylamine (122 µL, 0.87 mmol). The vial was sealed and the dark brown solution was heated at 100 ^{o}C for 6 hours, whereupon the reaction was cooled down to room temperature, diluted with CH_2Cl_2 (20 mL) and washed with water (2 x 20mL) and brine (20 mL). The organic layer was dried over Na_2SO_4, filtered, and concentrated under reduced pressure. The crude product was purified by column chromatography on silica gel using gradient elution from 20% CH_2Cl_2 in hexanes to 97% CH_2Cl_2 in hexanes. Product **16** was obtained as yellow thick oil (247 mg, 91%); analytical TLC on silica gel, 1:4 EtOAc/hexanes, R_f = 0.39. IR (film, cm^{-1}) 3309 (N–H), 1696 (C=O). ^{1}H NMR (400 MHz, $CDCl_3$, ppm) δ 7.67 – 7.62 (m, 2H), 7.49 – 7.45 (m, 3H), 7.43 – 7.35 (m, 4H), 7.12 (d, J = 1.5 Hz, 1H), 7.00 (dd, J = 7.8, 1.6 Hz, 1H), 6.77 (d, J = 7.9 Hz, 1H), 6.33 (d, J = 15.9 Hz, 1H), 5.25 (s, 2H), 4.81 (s, 1H). ^{13}C{^{1}H} NMR (100.6 MHz, $CDCl_3$, ppm) δ 167.2, 150.7, 145.1,

138.3, 136.3, 134.7, 130.3, 129.2, 128.7, 128.34, 128.33, 125.75, 125.73, 125.0, 122.8 (q, J = 288.0 Hz), 115.7, 111.3, 106.6, 98.3 (q, J = 32.4 Hz), 66.4. ^{19}F NMR (376.3 MHz, $CDCl_3$, ppm) δ -83.69. HRMS (ESI-TOF) *m/z*: $[M+H]^+$ Calcd for $C_{24}H_{19}F_3NO_3$ 426.1317; Found 426.1327.

3-(2-Phenyl-2-(trifluoromethyl)-2,3-dihydrobenzo[*d*]oxazol-6-yl)propanoic acid (11). To a yellow solution of benzyl (*E*)-3-(2-phenyl-2-(trifluoromethyl)-2,3-dihydrobenzo[*d*]oxazol-6-yl)acrylate (**15**) (379 mg, 0.89 mmol) in abs. EtOH (13 mL) was added 10% Pd–C (379 mg, 40 mol %) and H_2 gas was passed through the resulting suspension at room temperature for 2 hours. The progress of the hydrogenation was followed by UPLC-MS analysis. Once the reaction is completed, it was filtered through a plug of Celite. The filtrate was concentrated under reduced pressure to obtain the product that was used in the next step without additional purification. ^{1}H NMR (400 MHz, CD_3CN, ppm) δ 7.68 – 7.65 (m, 2H), 7.52 – 7.49 (m, 3H), 6.819 – 6.818 (m 1H), 6.75 – 6.70 (m, 2H), 5.53 (s, 1H), 2.81 (t, J = 7.6 Hz, 2H), 2.55 (s, J = 7.7 Hz, 2H). ^{13}C{^{1}H} NMR (100.6 MHz, CD_3CN, ppm) δ 174.4, 150.9, 136.2, 135.6, 135.4, 131.1, 129.8, 126.87, 126.86, 124.2, (q, J = 287.4 Hz), 122.8, 112.7, 109.3, 99.1 (q, J = 31.9 Hz), 36.0, 31.2. ^{19}F NMR (376.3 MHz, CD_3CN, ppm) δ –84.56. HRMS (ESI-TOF) *m/z*: $[M+H]^+$ Calcd for $C_{17}H_{15}F_3NO_3$ 338.1004; Found 338.1008.

2-Phenyl-2-(trifluoromethyl)-3',4'-dihydro-2*H*,5'*H*-spiro[benzo[*d*]oxazole-6,2'-furan]-5'-one (12) was obtained according to general procedure D from 3-(2-phenyl-2-(trifluoromethyl)-2,3-dihydrobenzo[*d*]oxazol-6-yl)propanoic acid (**11**). Purification by silica gel column chromatography using gradient elution from 9% EtOAc in hexanes to 33% EtOAc in hexanes afforded **12** as a 1:1 mixture of diastereomers (55 mg of red oil, 55%); analytical TLC on silica gel, 1:4 EtOAc/hexanes, R_f = 0.16. IR (film, cm^{-1}) 1784 (C=O), 1639 (C=N). HRMS (ESI-TOF) *m/z*: $[M+H]^+$ Calcd for $C_{17}H_{13}F_3NO_3$ 336.0848; Found 336.0848.

Individual pure diastereomers were obtained by preparative HPLC using isocratic elution with 20% EtOAc in hexanes as a mobile phase.

*Diastereomer **12a**:* ^{1}H NMR (400 MHz, $CDCl_3$, ppm) δ 7.74 – 7.72 (m, 2H), 7.46 – 7.42 (m, 3H), 6.77 (d, J = 9.9 Hz, 1H), 6.62 (dd, J = 9.9, 2.2 Hz, 1H), 5.54 (d, J = 2.1 Hz, 1H), 2.74 (td, J = 8.3, 1.6 Hz, 2H),

2.34 – 2.29 (m, 2H). $^{13}C\{^{1}H\}$ NMR (100.6 MHz, $CDCl_3$, ppm) δ 175.2, 159.7, 153.2, 145.3, 132.6, 130.3, 128.6, 127.6, 122.2 (q, J = 286.1 Hz), 120.4, 111.4 (q, J = 30.9 Hz), 100.7, 83.4, 34.5, 28.5. ^{19}F NMR (376.3 MHz, $CDCl_3$) δ -80.13.

*Diastereomer **12b***: ^{1}H NMR (400 MHz, $CDCl_3$, ppm) δ 7.73 – 7.70 (m, 2H), 7.46 – 7.42 (m, 3H), 6.77 (d, J = 9.8 Hz, 1H), 6.62 (dd, J = 9.8, 2.1 Hz, 1H), 5.54 (d, J = 2.1 Hz, m, 1H), 2.76 (td, J = 8.4, 2.3 Hz, 1H), 2.43 – 2.39 (m, 2H). $^{13}C\{^{1}H\}$ NMR (100.6 MHz, $CDCl_3$, ppm) δ 175.2, 159.8, 153.0, 145.4, 133.3, 130.3, 128.6, 127.6, 122.1 (q, J = 286.2 Hz), 120.7, 111.5 (q, J = 31.2 Hz), 100.9, 83.3, 34.4, 28.5. ^{19}F NMR (376.3 MHz, $CDCl_3$) δ –80.23.

Computational methods The presented theoretical considerations of the electrochemical cyclization of phenolic imines are predicated on calculations of a model system that comprises one substrate molecule with R^1 = H and R^2 = Ph (**7a**), one model iodine (III) molecule **13** (see also ref. 34) and one additional solvent (HFIP) molecule as depicted in Figure 5. The application of the model system shown in Figure 1 serves the dual purpose of retaining a constant number of nuclei and electrons throughout the entire reaction and stabilizing transitory charges by the extra solvent molecule. Moreover, as discussed above, the presence of at least one explicit solvent molecule is required as impetus for critical structural rearrangements. Nevertheless, it should be noted that the benefit of having a constant number of nuclei and electrons comes at the cost of underestimating the translation contributions to the enthalpy and entropy. In reality, each generated molecule, such as the released HFIP from **2**, gives rise to three translational degrees of freedom whereas in the quantum chemical description of the applied model system the number of translational degrees of freedom is constantly three. While the effect of this underestimation is small for all reaction steps that leave the number of independent molecules constant it is more pronounced during the reduction of iodine where the number of molecules in the model is increased by two. In this regard, we just note in passing that the effect will act to stabilize the product side of the reaction.

All quantum chemical calculations presented in this work have been conducted with the ORCA program package in its version 3.0 and employed the TPSS functional.[51] The considerable scalar relativistic effects arising from the presence of iodine are taken into account by the zero'th order regular approximation (ZORA).[52] Accordingly, the scalar-relativistically recontracted form of the def2-TZVP basis set was used.[53] Solvent effects that are not covered by the explicitly incorporated solvent molecule are modeled by the conductor-like screening model (COSMO) with a dielectric constant of $\varepsilon = 17.8$.[54] The generation of Coulomb integrals was accelerated by the well-established resolution of identity (RIJ) scheme together with the auxiliary basis set introduced by Weigend in 2006 (def2/J).[55] Dispersion effects were described using the semiempirical pairwise correction scheme by Grimme in its formulation of 2010 with Becke-Johnson damping (D3BJ).[56] Efficient numerical integration was ensured by using a dense integration grid (ORCA Grid 4). Harmonic vibrational frequencies were calculated numerically to verify the nature of the stationary points. Minimum energy points correspond to exclusively positive eigenvalues of the Hessian matrix while transition states feature one negative eigenvalue. Thermochemical contributions were calculated using the ideal gas, rigid rotor and harmonic oscillator approximations at a temperature of 298.15 K.

AUTHOR INFORMATION

Corresponding Authors

*E-mail: robert.francke@uni-rostock.de.

*E-mail: michael.roemelt@theochem.ruhr-uni-bochum.de

*E-mail: edgars@osi.lv

ORCID:

Robert Francke: 0000-0002-3752-2852

Edgars Suna: 0000-0002-3078-0576

Notes: The authors declare no competing financial interest.

ACKNOWLEDGMENTS

The work was in part funded by the German Research Foundation (DFG, grant no. FR 3848/1-1) and by Latvian Science Council (grant 274/2012). O. K. thanks INNOVABALT project for funding. R. F. is particularly grateful for a Liebig Fellowship (Fonds der Chemischen Industrie). M. R. gratefully acknowledges funding from the Otto-Hahn award program of the Max-Planck society.

ASSOCIATED CONTENT

Supporting Information

The following files are available free of charge on the ACS Publications website at DOI: 10.1021/acs.joc.XXXXXXX.

Photography of the electrochemical cell, Cartesian coordinates and NMR spectra (PDF)

REFERENCES

1. (a) Zhdankin, V. V.; Stang, P. J. *Chem. Rev.* **2008**, *108*, 5299–5358. (b) Zhdankin, V. V. *ARKIVOC* **2009**, 1–62. (c) Yoshimura, A.; Zhdankin, V. V. *Chem. Rev.* **2016**, *116*, 3328–3435. (d) Sun, C.-L.; Shi, Z.-J. *Chem. Rev.* **2014**, *114*, 9219–9280.
2. (a) Singh, F.; Wirth, T. *Synthesis* **2013**, *45*, 2499–2511. (b) Brown, M.; Kumar, R.; Rehbein, J.; Wirth, T. *Chem. Eur. J.* **2016**, *22*, 4030–4035.
3. (a) Martínez, C.; Wu, Y.; Weinstein, A. B.; Stahl, S. S.; Liu, G.; Muñiz, K. *J. Org. Chem.* **2013**, *78*, 6309–6315. (b) Liu, G.; Stahl, S. S. *J. Am. Chem. Soc.* **2006**, *128*, 7179–7181.
4. For selected reviews on I(III)-catalyzed transformations, see (a) Richardson, R. D.; Wirth, T. *Angew. Chem. Int. Ed.* **2006**, *45*, 4402–4404. (b) Ochiai, M.; Miyamoto, K. *Eur. J. Org. Chem.* **2008**, 4229–4239. (c) Dohi, T.; Kita, Y. *Chem. Commun.* **2009**, 2073–2085. (d) Dohi, T. *Chem. Pharm. Bull.* **2010**, *58*, 135–142. (e) Singh, F. V.; Wirth, T. *Chem. Asian J.* **2014**, *9*, 950–971. (f) Liu, D.; Lei, A. *Chem.–Asian J.* **2015**, *10*, 806–823.
5. For selected recent examples, see: (a) Dohi, T.; Maruyama, A.; Minamitsuji, Y.; Takenaga, N.; Kita, Y. *Chem. Commun.* **2007**, 1224–1226. (b) Antonchick, A. P.; Samanta, R.; Kulikov, K.; Lategahn, J. *Angew. Chem. Int. Ed.* **2011**, *50*, 8605–8608. (c) Morimoto, K.; Sakamoto, K.; Ohshika, T.; Dohi, T.; Kita, Y. *Angew. Chem. Int. Ed.* **2016**, *55*, 3652–3656. (d) Reitti, M.; Villo,

P.; Olofsson, B. *Angew. Chem. Int. Ed.* **2016**, *55*, 8928–8932. (e) Muñiz, K.; Barreiro, L.; Romero, R. M.; Martínez, C. *J. Am. Chem. Soc.* **2017**, *139*, 4354–4357.

6. For a review on indirect electrosynthesis, see (a) Francke, R.; Little, R. D. *Chem. Soc. Rev.* **2014**, *43*, 2492–2521. For recent outstanding applications of redox mediators in electrosynthesis, see (b) Qian, X-Y; Li, S.-Q.; Song, J.; Xu, H.-C. *ACS Catal.* **2017**, *7*, 2730–2734. (c) Hou, Z.-W.; Mao, Z.-Y.; Zhao, H.-B.; Melcamu, Y. Y.; Lu, X.; Song, J.; Xu, H.-C. *Angew. Chem. Int. Ed.* **2016**, *55*, 9168–9172. (d) Röse, P.; Emge, S.; König, C. A.; Hilt, G. *Adv. Synth. Catal.* **2017**, *359*, 1359–1372. (e) Jiang, Y.-Y.; Liang, S.; Hu, L.-M.; Little, R. D.; Zeng, C.-C. *J. Org. Chem.* **2016**, *81*, 4713-4719. (f) Kang, L.-S.; Luo, M-H.; Lam, C. M.; Hu, L.; Little, R. D.; Zeng, C-C. *Green Chem.* **2016**, *18*, 3767–3774. (g) Qian, P.; Su, J.-H.; Wang, Y.; Bi, M.; Zha, Z.; Wang, Z. *J. Org. Chem.* **2017**, *82*, 6434−6440. (h) Li, Y.; Gao, H.; Zhang, Z.; Qian, P.; Bi, M.; Zha. Z.; Wang, Z. *Chem. Commun.* **2016**, *52*, 8600−8603.
7. For selected synthetic applications of electrogenerated I(III) reagents, see: (a) Fuchigami, T.; Fujita, T. *J. Org. Chem.* **1994**, *59*, 7190–7192. (b) T. Fujita, T. Fuchigami, *Tetrahedron Lett.* **1996**, *37*, 4725–4728. (c) Inoue, K.; Ishikawa, Y.; Nishiyama, S. *Org. Lett.* **2010**, *12*, 436–439. (d) Kajiyama, D.; Inoue, K.; Ishikawa, Y.; Nishiyama, S. *Tetrahedron* **2010**, *66*, 9779–9784. Watts, K.; Gattrell, W.; Wirth, T. *Beilstein J. Org. Chem.* **2011**, *7,* 1108–1114.
8. Sawamura, T.; Kuribayashi, S.; Inagi, S.; Fuchigami, T. *Org. Lett.* **2010**, *12*, 644–646.
9. Sawamura, T.; Kuribayashi, S.; Inagi, S.; Fuchigami, T. *Adv. Synth. Catal.* **2010**, *352*, 2757–2760.
10. Broese, T.; Francke, R. *Org. Lett.* **2016**, *18*, 5896–5899.
11. Francke, R. *Beilstein J. Org. Chem.* **2014**, *10*, 2858–2873.
12. (a) Ovenden, S. P. B.; Nielson, J. L.; Liptrot, C. H.; Willis, R. H.; Tapiolas, D. M.; Wright, A. D.; Motti, C. A. *J. Nat. Prod.* **2011**, *74*, 65–68. (b) Yang, M.; Yang, X.; Sun, H.; Li, A. *Angew. Chem., Int. Ed.* **2016**, *55*, 2851-2855.
13. Demmer, C. S.; Bunch, L. *Eur. J. Med. Chem.* **2015**, *97*, 778–785.
14. (a) Rajasekhar, S.; Maiti, B.; Chanda, K. *Synlett* **2017**, *28*, 521–541. (b) Yu, C.; Guo, X.; Xi, Z.; Muzzio, M.; Yin, Z.; Shen, B.; Li, J.; Seto, C. T.; Sun, S. *J. Am. Chem. Soc.* **2017**, *139*, 5712−5715. (c) Nguyen, T. B.; Retailleau, P. *Org. Lett.* **2017**, *19*, 3887–3890.
15. Gieshoff, T.; Kehl, A.; Schollmeyer, D.; Moeller, K. D.; Waldvogel, S. R. *Chem Commun* **2017**, *53*, 2974–2977.
16. Morofuji, T.; Shimizu, A.; Yoshida, J. *Chem. - Eur. J.* **2015**, *21*, 3211–3214.
17. (a) Shih, Y.; Ke, C.; Pan, C.; Huang, Y. *RSC Adv.* **2013**, *3*, 7330-7336. (b) There is a single example for electrochemical synthesis of benzoxazole (40% yield) from benzylic alcohol and

ortho-aminophenol in the presence of Co(II) salts: Lai, Y.-L.; Ye, J.-S.; Huang, J.-M. *Chem. - Eur. J.* **2016**, *22*, 5425–5429.

18. Kang, L.-S.; Xiao, H.; Zeng, C.-C.; Hu, L.-M.; Little, R. D. *J. Electroanal. Chem.* **2016**, *767*, 13–17.
19. Li, W.-C.; Zeng, C.-C.; Hu, L.-M.; Tian, H.-Y.; Little. R. D. *Adv. Synth. Catal.* **2013**, *355*, 2884–2890.
20. Stoichiometric amounts of I(III) reagents have been employed for the oxidative cyclization of *ortho*-iminophenols to benzoxazoles: (a) Varma, R. S.; Saini, R. K.; Prakash, O. *Tetrahedron Lett.* **1997**, *38*, 2621–2622. (b) Zhang, J.-Z.; Zhu, Q.; Huang, X. *Synth. Commun.* **2002**, *32*, 2175–2179. (c) Naganaboina, R. T.; Peddinti, R. K. *Tetrahedron* **2015**, *71*, 6245–6253.
21. (a) Tohma, H.; Takizawa, S.; Maegawa, T.; Kita, Y. *Angew. Chem. Int. Ed.* **2000**, *39*, 1306–1308. (b) Tohma, H.; Maegawa, T.; Takizawa, S.; Kita, Y. *Adv. Synth. Catal.* **2002**, *344*, 328–337. (c) Dohi, T.; Maruyama, A.; Yoshimura, M.; Morimoto, K.; Tohma, H.; Shiro, M.; Kita, Y. *Chem Commun.* **2005**, 2205–2207.
22. The published oxidation of *sec*-alcohols to ketones by I(III) reagents required the use of KBr as an additive: see ref. 21.
23. Ochiai, M. *Top. Curr. Chem.* **2003**, *224*, 6-67.
24. Intermolecular β-elimination is less likely mechanistic scenario as it requires dissociation of highly basic HFIP-derived alkoxide from the tetracoordinated iodate **6**.
25. Attempts to prepare **2** using various oxidizing agents were not successful. Thus, treatment of **1** with excess sodium peroxysulfate or excess H_2O_2 (30% aqueous solution) in HFIP did not lead to any conversion, whereas the use of MCPBA (2 equiv.) afforded **2** together with substantial amounts of an unidentified side-product.
26. Since both species are oxidized irreversibly, peak potentials E_P are reported instead of the equilibrium potentials E_0.
27. (a) Nitro-substituted imines were not suitable as substrates in DDQ and NaI-mediated electrocyclizations: see refs 18 and 19. (b) Preliminary experiments evidence that the electrochemically generated I(III) reagent **2** is also suitable for the cyclization of 2-(benzylideneamino)thiophenols to benzothiazoles.
28. Said, G.; Grippon, S.; Kirkpatrick, P. *Nat. Rev. Drug. Discov.* **2012**, *11*, 185–186.
29. (a) Dohi, T.; Yamaoka, N.; Kita, Y. *Tetrahedron* **2010**, *66*, 5775–5785. (b) Dohi, T.; Ito, M.; Yamaoka, N.; Morimoto, K.; Fujioka, H.; Kita, Y. *Angew. Chem. Int. Ed.* **2010**, *49*, 3334–3337.
30. Sokolovs, I.; Lubriks, D.; Suna, E. *J. Am. Chem. Soc.* **2014**, *136*, 6920–6928.
31. Franz, J. A.; Barrows, R. D.; Camaioni, D. M. *J. Am. Chem. Soc.* **1984**, *106*, 3964–3967.

32. Dohi, T.; Uchiyama, T.; Yamashita, D.; Washimi, N.; Kita, Y. *Tetrahedron Lett.* **2011**, *52,* 2212-2215.
33. The formation of **V** is also possible directly from imine **7a–A** and **2** without involvement of cyclic tautomer **7a–B**. Accordingly, an interaction of Lewis basic imine nitrogen in **7a–A** with Lewis acidic I(III) center facilitates cyclization to **V** with concomitant formation of HFIP (see ref. 20a).
34. It was assumed that the presence of ammonium group and its ClO_4^- counterion in the aliphatic chain of the mediator **2** have no influence on the cyclization reaction. Therefore, the charged moiety has been omitted in the model to reduce the computational costs (see structure **13**, Figure 5).
35. Of course, the applied computational model is unfit to yield any reasonable estimates of the rates at which such a movement occurs or its associated barriers. An adequate description of this event would require a full molecular dynamics simulation that explicitly includes many shells of solvent molecules. Such a molecular dynamics simulation is out of scope of this work and from our perspective not worthwhile regarding the limited relevance of this step for the overall reaction mechanism. We believe it is safe to assume that at room temperature, the anion itself or at least its negative charge is sufficiently mobile in the HFIP solution to readily undergo the required motion at sufficiently high rates.
36. Zhao, X.-F.; Zhang, C. *Synthesis* **2007**, 551–557.
37. Wang, L.; Ma, Z.-G.; Wie X.-J.; Meng, Q.-Y., Yang, D.-T; Du., S.-F.; Chen, Z.-F., Wu, L.-Z.; Liu, Q. *Green Chem.* **2014**, *16*, 3752–3757.
38. Chen, C.-L.; Liu, Y.-H.; Peng, S.-M.; Liu, S.-T. *J. Organomet. Chem.* **2004**, *689*, 1806–1815.
39. Cho, Y. H.; Lee, C.-Y.; Ha, D.-C.; Cheon, C.-H. *Adv. Synth. Catal.* **2012**, *354*, 2992–2996.
40. Mas-Montoya, M.; Usea, L.; Ferao, A. E.; Montenegro, M. F.; Ramírez de Arellano, C.; Tarraga, A.; Rodríguez-Lopez, J. N.; Curiel, D. *J. Org. Chem.* **2016**, *81*, 3296–3302.
41. Bae, S. J.; Ha, Y. M.; Park, Y. J.; Park, J. Y.; Song, Y. M.; Ha, T. K.; Chun, P.; Moon, H. R.; Chung, H. Y. *Eur. J. Med. Chem.* **2012**, *57*, 383–390.
42. Peacock, L. R.; Chapman, R. S. L.; Sedgwick, A. C.; Mahon, M. F.; Amans, D.; Bull, S. D. *Org. Lett.* **2015**, *17*, 994–997.
43. Park, H. J.; Park, M. S.; Lee, T. H. *J. Heterocycl. Chem.* **2013**, *50*, 663–667.
44. Chi, Y.-H.; Lee, C.-Y.; Cheon, C.-H. *Tetrahedron* **2013**, *69*, 6565–6573.
45. Yang, K.; Wang, P.; Zhang, C.; Kadi, A. A.; Fun, H.-K.; Zhang, Y.; Lu, H. *Eur. J. Org. Chem.* **2014**, 7586–7589.
46. Zhu, F.; Wang, Z.-X. *Org. Lett*. **2015**, *17*, 1601–1604.

47. Meng, L.; Kamada, Y.; Muto, K.; Yamaguchi, J.; Itami, K. *Angew. Chem., Int. Ed.* **2013**, *52*, 10048–10051.
48. Liu, S.; Chen, R.; Guo, X.; Yang, H.; Deng, G.; Li, C.-J. *Green Chem*. **2012**, *14*, 1577–1580.
49. Tan, H.; Pan, C.-X; Xu, Y.-L.; Wang, H.-S.; Pan, Y.-M. *J. Chem. Res.* **2012**, *36*, 370–373.
50. Ohkata, K.; Tamura, Y.; Shetuni, B. B.; Takagi, R.; Miyanaga, W.; Kojima, S.; Paquette, L. A. *J. Am. Chem. Soc.* **2004**, *126*, 16783–16792.
51. (a) Neese, F. *WIREs Comput. Mol. Sci.* **2012**, *2*, 73–78. (b) Tao, J.; Perdew, J. P.; Staroverov, V. N.; Scuseria, G. E. *Phys. Rev. Lett.* **2003**, *91*, 146401-1–146401-4.
52. (a) Lenthe, E. v.; Baerends, E. J.; Snijders, J. G. *J. Chem. Phys.* **1993**, *99*, 4597–4610. (b) van Wüllen, C. *J. Chem. Phys*. **1998**, *109*, 392–399.
53. (a) Weigend, F.; Ahlrichs, R. *Phys. Chem. Chem. Phys*. **2005**, *7*, 3297–3305. (b) Pantazis, D.; Chen, X.; Landis, C.; Neese, F. *J. Chem. Theory Comput.* **2008**, *4*, 908–919.
54. (a) Klamt, A.; Schüürmann, G. *J. Chem. Soc. Perkin. Trans*. **1993**, *2*, 799–805. (b) Hong, D.-P.; Hoshino, M.; Kuboi, R.; Goto, Y. *J. Am. Chem. Soc.* **1999**, *121*, 8427–8433.
55. (a) Whitten, J. L. *J. Chem. Phys.* **1973**, *58*, 4496–4501. (b) Dunlap, B. I.; Connolly, J. W. D.; Sabin, J. R. *J. Chem. Phys*. **1979**, *71*, 3396–3402. (c) Vahtras, O.; Almlöf, J.; Feyereisen, M. W. *Chem. Phys. Lett.* **1993**, *213*, 514–518. (d) Neese, F. *J. Comput. Chem.* **2003**, *24*, 1740–1747. (e) Weigend, F. *Phys. Chem. Chem. Phys*. **2006**, *8*, 1057–1065.
56. (a) Grimme, S.; Antony, J.; Ehrlich, S.; Krieg, H. *J. Chem. Phys.* **2010**, *132*, 154104-1–154104-19. (b) Grimme, S.; Ehrlich, S.; Goerigk, L. *J. Comput. Chem.* **2011**, *32*, 1456–1465.